Mild P–P Bond Cleavage in the Methyldiphosphenyl Complex $[Mo_2Cp_2(\mu\text{-}PCy_2)(\mu\text{-}\kappa^2\text{:}\kappa^2\text{-}P_2Me)(CO)_2]$ to Give Novel Phosphide-Bridged Trinuclear Derivatives.

M. Angeles Alvarez,[a] M. Esther García,[a] Daniel García-Vivó,[a] Raquel Lozano,[a] Alberto Ramos,[b]* and Miguel A. Ruiz[a]*

[a] *Departamento de Química Orgánica e Inorgánica / IUQOEM, Universidad de Oviedo, E-33071 Oviedo, Spain.*

[b] *Instituto Nacional del Carbón, CSIC, Francisco Pintado Fe 26, E-33011 Oviedo, Spain.*

Abstract

Reactions of the title diphosphenyl complex with $[Fe_2(CO)_9]$ and $[W(CO)_4(THF)_2]$ gave the trinuclear species $[Mo_2FeCp_2(\mu_3\text{-}P)(\mu\text{-}PCy_2)(\mu_3\text{-}PMe)(CO)_5]$ and $[Mo_2WCp_2(\mu_3\text{-}P)(\mu\text{-}PCy_2)(\mu_3\text{-}PMe)(CO)_6]$ following from formal insertion of the 14-electron fragments $Fe(CO)_3$ and $W(CO)_4$, respectively, in the P–P bond of the diphosphenyl ligand and formation of a new heterometallic bond (Mo–Fe = 2.9294(6) and Mo–W = 3.146(1) Å). Reactions of the diphosphenyl complex with the tetrahydrofuran adducts $[ML_n(THF)]$ (ML_n = $MnCp'(CO)_2$, $W(CO)_5$) led instead to trinuclear diphosphenyl complexes $[Mo_2MCp_2Cp'(\mu\text{-}PCy_2)(\mu_3\text{-}\kappa^2\text{:}\kappa^2\text{:}\kappa^1\text{-}P_2Me)(CO)_2L_n]$ following from coordination in each case of the corresponding 16-electron fragment ML_n to the lone-pair-bearing P atom of the P_2Me ligand. However, these diphosphenyl complexes were unstable, and decomposed at room temperature or under mild heating by releasing methylphosphinidene (PMe), to give the corresponding derivatives $[Mo_2MCp_2(\mu_3\text{-}P)(\mu\text{-}PCy_2)(CO)_2L_n]$ displaying planar trigonal phosphide ligands giving rise to strongly deshielded ^{31}P NMR resonances (δ_P ca. 1100 ppm), while being involved in strong π bonding with the unsaturated Mo_2 center of these molecules (Mo–Mo = 2.749(1) Å and Mo–P ca. 2.30 Å when M = W). An isolobal analogy could be established between the $P\rightarrow ML_n$ fragments in these products and a carbyne ligand (CR), supported by density functional calculations on the tungsten compound, which also enabled an easy interpretation and prediction of their chemical behavior. Thus the manganese complex could be reversibly carbonylated (p_{CO} ca. 3 atm, 293 K) to give the corresponding electron-precise pentacarbonyl $[MnMo_2Cp_2Cp'(\mu_3\text{-}P)(\mu\text{-}PCy_2)(CO)_5]$ (Mo–Mo = 3.1318(7) Å), a process also involving a *trans* to *cis* rearrangement of the Mo_2Cp_2 subunit. On the other hand, decarbonylation of the tungsten complex was accomplished in refluxing toluene solution to give the hexacarbonyl $[Mo_2WCp_2(\mu_3\text{-}P)(\mu\text{-}PCy_2)(\mu\text{-}CO)(CO)_5]$, a derivative containing an unsaturated 30-electron dimolybdenum center with an intermetallic triple bond.

Introduction

We recently described the preparation of the methyldiphosphenyl complex $[Mo_2Cp_2(\mu\text{-}PCy_2)(\mu\text{-}\kappa^2\text{:}\kappa^2\text{-}P_2Me)(CO_2)]$ (**1**) through the room-temperature reaction of MeI with the anionic diphosphorus complex $[Mo_2Cp_2(\mu\text{-}PCy_2)(\mu\text{-}\kappa^2\text{:}\kappa^2\text{-}P_2)(CO)_2]^-$, a molecule prepared in turn through the symmetrical cleavage of white phosphorus (P_4) by the unsaturated dimolybdenum complex $[Mo_2Cp_2(\mu\text{-}PCy_2)(\mu\text{-}CO)_2]^-$ under mild conditions (Scheme 1).[1]

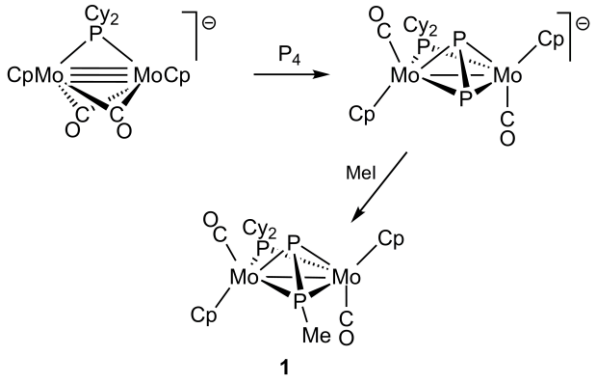

Scheme 1

Among the family of reported diphosphenyl complexes, compound **1** represents an unique example of a complex displaying a P_2R ligand symmetrically bridging two metal atoms (type **D** in Chart 1), since the most common coordination mode for this ligand is the terminal κ^1 mode found in mononuclear compounds (type **A** in Chart 1).[2] There are also some examples of μ_2-P_2R complexes with other arrangements of the bridging ligand, generally derived from reactions of a parent mononuclear κ^1-diphosphenyl complex with different metal fragments. Most of these reactions involve the lone pair (LP) of the metal-bound P atom to give a *P*,*P*-bridged derivative (type **B** coordination), as found in the reactions of $[MCp^*(NO)(CO)(\kappa^1\text{-}P_2Mes^*)]$ (M = Mn, Re; Mes* = 2,4,6-$C_6H_2{}^tBu_3$) with a $Cr(CO)_5$ fragment to give $[CrMCp^*(\mu\text{-}\kappa^1\text{:}\kappa^1\text{-}P_2Mes^*)(NO)(CO)]$.[3] Alternatively, the terminal complex can bind a second metal fragment through its double P–P bond to give a *P*:*P*,*P*′-bridged derivative (type **C** coordination), as observed in the reaction of $[FeCp^*(CO)_2(\kappa^1\text{-}P_2Mes^*)]$ with a $Pt(PPh_3)_2$ moiety to give $[FePtCp^*(\mu\text{-}\kappa^1\text{:}\kappa^2\text{-}P_2Mes^*)(CO)_2(PPh_3)_2]$.[4] Finally, a few examples of μ_3-P_2R complexes have been also reported, these involving the participation of both P-based LPs and also the double P–P bond for binding to the metal atoms, as found in the triiron complexes $[Fe_3Cp_3(CO)_2(\mu_3\text{-}\kappa^1\text{:}\kappa^2\text{:}\kappa^1\text{-}P_2{}^tBu)(\mu_3\text{-}P^tBu)]$ (type **E**),[5] $[Fe_3Cp^*(\mu_3\text{-}\kappa^1\text{:}\kappa^1\text{:}\kappa^2\text{-}P_2{}^tBu)(CO)_{10}]$ (type **F**),[6] and $[Fe_3Cp^*(\mu_3\text{-}\kappa^1\text{:}\kappa^2\text{:}\kappa^2\text{-}P_2{}^tBu)(CO)_8]$ (type **G**).[6]

Chart 1

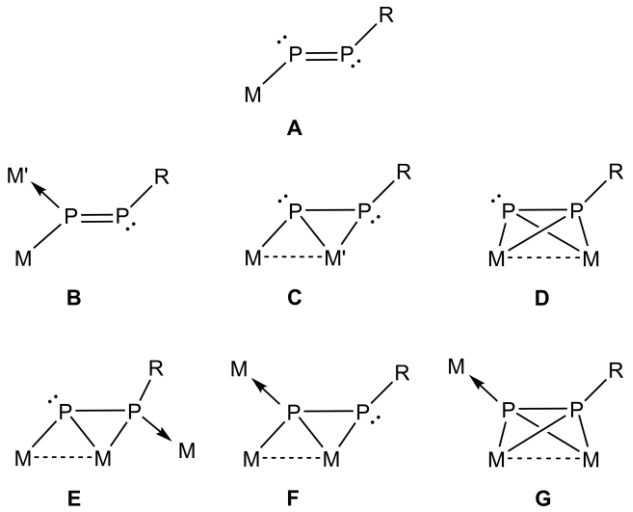

Complexes of types **F** and **G** can be obviously related to those of types **C** and **D** respectively, and expected to be formed from the latter ones upon additional coordination of a 16-electron metal fragment through the LP at the bridgehead phosphorus atom. Unfortunately, the behavior of complexes with bridging diphosphenyl ligands has been little explored to date, and the outcome of these seemingly simple reactions might not be so straightforward. In particular, reactions of a type **D** diphosphenyl complex with an unsaturated metal fragment might involve P–P cleavage (or insertion) processes. Precedents for such possible outcomes can be found in the reaction of the μ_3-diphosphenyl complex $[Fe_3Cp^*(\mu_3\text{-}\kappa^2\text{:}\kappa^2\text{:}\kappa^1\text{-}P_2{}^t\text{Bu})(CO)_8]$ with $[Fe_2(CO)_9]$ to give $[Fe_3Cp^*\{\mu_3\text{-}\kappa^2\text{:}\kappa^2\text{:}\kappa^1\text{-}PC(O)P^t\text{Bu}\}(CO)_8]$, the latter following from insertion of a CO molecule in the P–P bond of the diphosphenyl ligand,[6] and in the room temperature reaction of the diphosphorus-bridged complex $[Re_2Cp^*_2(\mu\text{-}\kappa^2\text{:}\kappa^2\text{-}P_2)(CO)_4]$ (a molecule related to diphosphenyl complexes of type **D**) with $[W(CO)_5(THF)]$ to give, *inter alia*, a phosphide complex $[W_2Re_2Cp^*_2(\mu_3\text{-}P)_2(CO)_{12}]$ derived from insertion of the tungsten fragment in the P–P bond of the diphosphorus ligand.[7] Since the cleavage of P–P bonds in this sort of ligands is a matter of general interest in the context of P_4 activation by transition-metal complexes,[8] and recalling that eventually compound **1** is derived itself from white phosphorus, we considered of interest to explore the reactivity of our diphosphenyl complex with different precursors of 14- and 16-electron metal carbonyl fragments. These reactions, however, proved to be rather complex and strongly dependent on stoichiometry and reaction conditions, and we here report on those reactions incorporating a single metal fragment, while those leading to tetranuclear derivatives of **1** will be reported separately.[9] As it will be shown below, all reactions incorporating a single metal-fragment eventually involve the cleavage of the P–P bond in the diphosphenyl ligand of **1** under mild conditions, to

yield derivatives containing phosphide and methylphosphinidene ligands, with the latter being sometimes de-coordinated along the process.

Results and Discussion

Incorporation of 14-Electron Metal Fragments. Compound **1** reacted readily at room temperature with stoichiometric amounts of $[Fe_2(CO)_9]$ to give the trinuclear phosphide methylphosphinidene complex $[Mo_2FeCp_2(\mu_3\text{-}P)(\mu\text{-}PCy_2)(\mu_3\text{-}PMe)(CO)_5]$ (**2a**), formally derived from addition of the 14-electron fragment $Fe(CO)_3$ to a MoP_2 face of the Mo_2P_2 tetrahedral core of **1** with full scission of the P–P bond (Scheme 2). Analogously, reaction of **1** with a freshly prepared solution of the tetrahydrofuran adduct $[W(CO)_4(THF)_2]$ gave $[Mo_2WCp_2(\mu_3\text{-}P)(\mu\text{-}PCy_2)(\mu_3\text{-}PMe)(CO)_6]$ (**2d**), a trinuclear cluster displaying a structure comparable to that of **2a**, as discussed below, and following analogously from formal addition of the 14-electron fragment $W(CO)_4$ to a MoP_2 face of the core of **1** with P–P bond cleavage. This reaction, however, also gave small amounts of the type **G** diphosphenyl complex $[Mo_2WCp_2(\mu\text{-}PCy_2)(\mu_3\text{-}\kappa^2\text{:}\kappa^2\text{:}\kappa^1\text{-}P_2Me)(CO)_7]$ (**3d**) and the phosphide derivative $[Mo_2WCp_2(\mu_3\text{-}P)(\mu\text{-}PCy_2)(CO)_7]$ (**4d**). The latter side-products contain $W(CO)_5$ fragments and likely are derived from the presence of small amounts of the pentacarbonyl adduct $[W(CO)_5(THF)]$ in the corresponding reaction mixtures, as shown by separate experiments to be discussed later on (Scheme 2). On the other hand, we note that formation of the pentacarbonyl complex **2a** is itself somewhat unexpected since $[Fe_2(CO)_9]$ is a well-known precursor of the 16-electron fragment $Fe(CO)_4$, and therefore expected to lead to a type **G** derivative, as noted above. It is likely that such a derivative might be initially formed in the above reaction, then rapidly undergoing decarbonylation to yield **2a**, a matter to be discussed in more detail later on.

Scheme 2

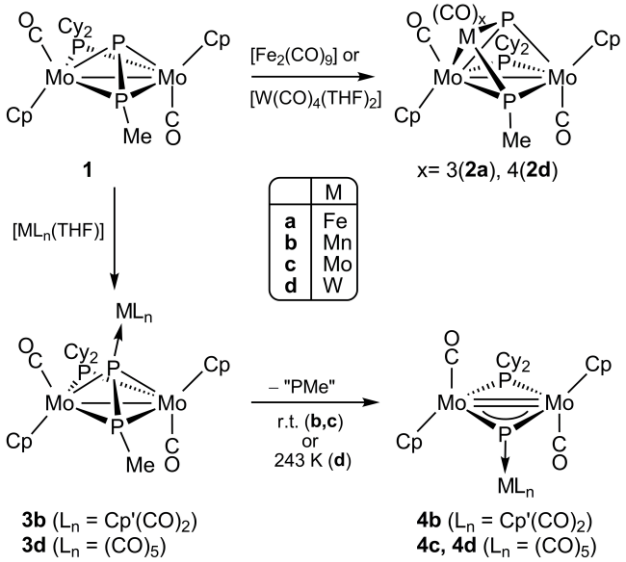

Solid-State Structure of Compounds 2a and 2d. The structure of **2a** in the crystal lattice (Figure 1 and Table 1) can be derived from that of the parent methyldiphosphenyl complex **1** after adding a pyramidal $Fe(CO)_3$ fragment to the Mo1–P2–P3 face of the tetrahedral Mo_2P_2 core of **1** with full cleavage of the P–P bond, as indicated by the long P–P separation of 2.672(1) Å (cf. 2.085(1) Å in **1**),[2] thus giving rise to new phosphinidene (PMe) and phosphide (P) ligands, both of them triply bridging the resulting V-shaped Mo_2Fe metal core. The somewhat distorted transoid arrangement of the Mo-bound Cp and CO ligands, denoted by the quite different Mo–Mo–CO angles of 116.2(1) and 83.5(1)º, is reminiscent of that found in the parent complex **1** and related derivatives of the anion $[Mo_2Cp_2(\mu\text{-}PCy_2)(\mu\text{-}\kappa^2\text{:}\kappa^2\text{-}P_2)(CO)_2]^-$,[1,10] probably caused here by the steric pressure induced by the apical P atom (P3) and the $Fe(CO)_3$ fragment on the CO ligand attached to Mo1, while the basal P atom (P2) remains placed close to the $Mo_2P(Cy)$ plane. The Mo–Mo bond distance of 2.9897(4) Å is consistent with the formulation of a single Mo–Mo bond, as required on the basis of the 18-electron rule for this molecule, and the same can be said of the Mo1–Fe1 separation of 2.9294(6) Å, which is comparable to that measured for the 34-electron complex $[FeMoCp(\mu\text{-}PCy_2)(CO)_6]$.[11]

The coordination of phosphide and methylphosphinidene ligands in **2a** deserves some comments. As for the first ligand, we note that most pyramidal μ_3-P complexes structurally characterized so far involve P atoms bridging metal triangles, and compounds **2a** and **2d** actually represent the first examples of V-shaped trinuclear clusters triply bridged by a phosphide ligand to be structurally characterized. The Mo–P(3) separations of 2.50 Å are only slightly shorter than the corresponding separations in **1** (ca. 2.53 Å) while the Fe–P(3) length (2.308(1) Å) is ca. 0.2 Å shorter, as expected from the difference in covalent radii of Mo and Fe atoms.[12] These separations are thus consistent with a formal description of the P atom as contributing with one electron to each of the metal atoms. For comparison, the phosphide ligands bridging triangular faces in the clusters $[W_6Cp^*_2(\mu_3\text{-}P)_2(\mu_4\text{-}P)_2(CO)_{16}]$,[13] and $[Mo_2WCp_2Cp^*(\mu_3\text{-}P)(CO)_6]$,[14] display M–P lengths in the range 2.39-2.52 Å.

In order to fulfill an 18-electron configuration around each metal center, however, the phosphinidene ligand should contribute with one electron to each Mo atom, and with two electrons to the Fe atom. This is in agreement with the quite short Fe1–P2 length of 2.176(1) Å, which falls in the range of distances found for compounds of formula $[Fe_2Cp_2(\mu\text{-}CO)_2(CO)(PR_3)]$ (2.13-2.21 Å) having classical two-electron P-donors.[15] Moreover, it might be anticipated that the lower coordination number of the Mo2 atom should be balanced with a stronger coordination of the PCy_2 ligand to that center, which is in agreement with the shorter P1–Mo2 length of 2.4289(8) Å (cf. 2.4852(8) Å for P1–Mo1), although the phosphinidene ligand also seems involved in the task, since it is

also placed significantly closer to the Mo2 atom (2.3665(9) vs. 2.4565(9) Å). We finally note the coordination environment of the phosphinidene P atom in **2a**, with the Me group almost placed in the Fe1P2Mo2 plane, thus configuring a geometry strongly departing from the more common tetrahedral environment of phosphorus. This geometry likely allows for a stronger interaction of phosphorus with the Fe1 and Mo2 atoms (recall the shorter lengths of these bonds), and is not unusual in 50-electron (hence V-shaped) trinuclear clusters bridged by phosphinidene ligands,[16] although it seems that no related clusters containing group 6 metals have been structurally characterized so far.

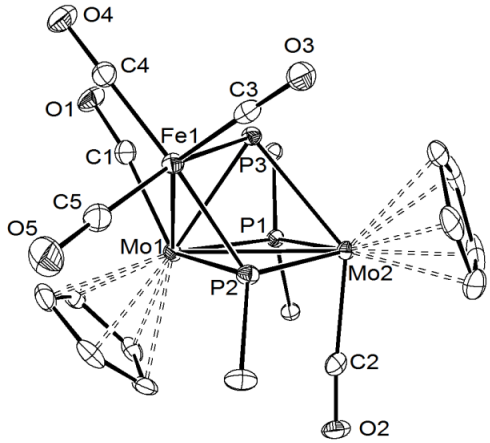

Figure 1. ORTEP diagram (30% probability) of compound **2a** with H atoms and Cy groups (except the C^1 atoms) omitted for clarity

Table 1. Selected Bond Lengths (Å) and Angles (°) for Compound **2a**.

Mo1–Mo2	2.9897(4)	C1–Mo1–Mo2	116.2(1)
Mo1–Fe1	2.9294(6)	C2–Mo2–Mo1	83.5(1)
Mo1–P1	2.4852(8)	P3–Mo1–P1	73.79(3)
Mo2–P1	2.4289(8)	P3–Mo2–P1	74.11(3)
Mo1–P2	2.4565(9)	P2–Mo1–P1	101.91(3)
Mo2–P2	2.3665(9)	P2–Mo2–P1	106.32(3)
Mo1–P3	2.4769(9)	P2–Mo1–P3	65.60(3)
Mo2–P3	2.5133(9)	P2–Mo2–P3	66.33(3)
Fe1–P2	2.176(1)	P2–Fe1–P3	73.10(3)
Fe1–P3	2.308(1)	Mo1–Fe1–P3	54.91(2)
Mo1–C1	1.965(4)	Mo1–Fe1–P2	55.17(3)
Mo2–C2	1.983(4)	C3–Fe1–C4	99.1(2)
Fe1–C3	1.766(4)	C3–Fe1–C5	102.6(2)
Fe1–C4	1.812(4)	C4–Fe1–C5	95.1(2)
Fe1–C5	1.785(4)		
P2–C6	1.859(4)		

The structure of **2d** in the crystal lattice is comparable to that of **2a** if we just replace the $Fe(CO)_3$ fragment with the isoelectronic $W(CO)_4$ one, therefore a detailed discussion is not needed. There are two independent molecules in the unit cell, quite similar to each other, and a view emphasizing the V-shaped metal core of one of the two molecules is shown in Figure 2, while the most relevant geometrical parameters are

collected in Table 2. As found for the iron cluster, the PCy_2 and PMe ligands are placed ca. 0.1 Å closer to the Mo atom having the lower coordination number (Mo1 here), and the phosphinidene ligand formally provides the tungsten atom with two electrons, in agreement with the very short W–P2 length of 2.409(1) Å (cf. 2.594(1) Å for W–P1). The newly formed Mo–W bond (3.146(1) Å) is longer than the PCy_2-bridged Mo–Mo bond (2.976(1) Å), but such intermetallic length still is fairly normal for a single bond. For comparison, the phosphinidene-bridged Mo–Mo bonds in the 48-electron clusters $[Mo_2MCp_2(\mu_3\text{-PPh})(CO)_7]$ (M = Fe, Ru) display comparable Mo–Mo lengths of ca. 3.17 Å.[17]

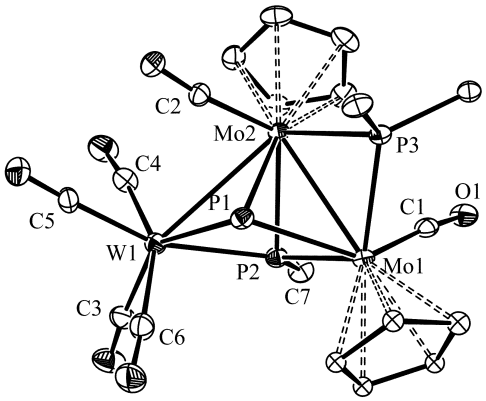

Figure 2. ORTEP diagram (30% probability) of one of the two independent molecules of compound **2d** in the unit cell, with H atoms and Cy groups (except the C^1 atoms) omitted for clarity.

Table 2. Selected Bond Lengths (Å) and Angles (º) for Compound **2d**

Mo1–Mo2	2.976(1)	C1–Mo1–Mo2	83.6(2)
Mo2–W1	3.146(1)	C2–Mo2–Mo1	117.5(1)
Mo1–P1	2.492(2)	P3–Mo1–P1	73.34(5)
Mo2–P1	2.452(1)	P3–Mo2–P1	72.51(4)
Mo1–P2	2.399(1)	P2–Mo1–P1	69.13(5)
Mo2–P2	2.526(1)	P2–Mo2–P1	67.75(5)
Mo1–P3	2.413(1)	P2–Mo1–P3	108.70(5)
Mo2–P3	2.501(1)	P2–Mo2–P3	102.08(4)
W1–P1	2.594(1)	P1–W1–P2	67.29(5)
W1–P2	2.409(1)	W1–P1–Mo1	106.18(5)
Mo1–C1	1.979(5)	W1–P1–Mo2	77.10(4)
Mo2–C2	1.993(5)	W1–P2–Mo1	115.53(5)
W1–C3	1.993(5)	W1–P2–Mo2	79.18(4)
W1–C4	2.042(5)	C3–W1–C4	83.5(2)
W1–C5	2.007(5)	C4–W1–C5	81.5(2)
W1–C6	2.021(5)	C3–W1–C5	107.7(2)
P2–C7	1.851(5)		

Solution Structure of Compounds 2a,d. The IR spectrum of compound **2a** in dichloromethane solution exhibits four C–O stretching bands at 2010, 1945, 1927 and 1892 cm^{-1} (Table 3). The first three bands can be attributed to a pyramidal $Fe(CO)_3$ oscillator in a low-symmetry environment,[18] and are comparable to those measured in the related clusters $[FeMo_2Cp_2(\mu_3\text{-X})(\mu\text{-}PCy_2)(CO)_5]$ (X = COMe, OMe),[19] or $[FeMo_2Cp_2(\mu\text{-}PPh_2)(\mu_3\text{-CCPh})(CO)_5]$.[20] The fourth band can be attributed to the

$Mo_2(CO)_2$ oscillator of the molecule, but the other band arising from this fragment cannot be identified in solution. This circumstance is not unusual in heterometallic clusters combining $Mo_2(CO)_2$ oscillators with $M(CO)_x$ ones (x = 3 to 5), and is due to the comparatively low intensity of the bands mainly arising from the former oscillator.[19] In fact, the IR spectrum of **2a** recorded in Nujol mull allows the identification of the two bands assignable to the $Mo_2(CO)_2$ fragment, which appear at 1868 (m) and 1829 (w, sh) cm^{-1}, in positions comparable to those of several heterometallic derivatives of the type $[Mo_2MCp_2(\mu\text{-}PCy_2)(\mu_3\text{-}\kappa^2\text{:}\kappa^2\text{:}\kappa^1\text{-}P_2)(CO)_2L_n]$ having structures comparable to that of **1**.[10] In the same line, we note that the IR spectrum of **2d** in solution exhibits only two bands of strong intensity at 2010 and 1911 cm^{-1}, which are clearly assignable to the C–O stretches of the $W(CO)_4$ fragment, while no bands at frequencies below 1900 cm^{-1} attributable to the $Mo_2(CO)_2$ oscillator are observed in this case.

The NMR spectra of compounds **2a,d** are essentially consistent with their solid-state structures. The $^{31}P\{^1H\}$ NMR spectra show in each case three distinct resonances corresponding to the PMe, P and PCy_2 ligands, respectively (Table 3). The phosphide and phosphinidene ligands display negligible mutual coupling, in agreement with the P–P bond cleavage operated on the former diphosphenyl ligand (cf. $^1J_{PP}$ = 503 Hz in **1**), and the PCy_2 ligand in **2a** displays moderate but distinct two-bond coupling to the PMe (14 Hz) and P (9 Hz) ligands, which are close to zero in the case of **2d**. The ^{31}P chemical shifts of ca. 300 ppm for the PMe ligands in **2a,d** are not very unusual for phosphinidene ligands bridging three metal atoms,[16,21,22] but the shifts of 239.2 and 124.5 ppm for the phosphide ligands in these clusters must be considered as rather low for a pyramidal μ_3-P ligand. For comparison, the phosphide bridging the trimetal core in the 48-electron clusters $[Mo_2MCp_3(\mu_3\text{-}P)(CO)_6]$ display chemical shifts of 560.3 and 459.0 ppm when M = Mo and W respectively.[23] Such relative shieldings in compounds **2** are likely derived from the fact that these molecules are V-shaped, 50-electron clusters rather than triangular, 48-electron clusters, and we notice that a similar shielding effect has been previously found for phosphinidene-bridged trinuclear clusters when going from 48- to 52-electron species.[16,22] We finally note that the ^1H and $^{13}C\{^1H\}$ NMR spectra of these compounds are generally consistent with the absence of any symmetry element in these molecules, except for the ^{13}C resonances of the heterometallic $M(CO)_n$ fragment, which in both cases appear as just a single resonance at 212.8 (Fe) or 215.9 ppm (W). This is indicative of the operation in solution of a dynamic process fast on the NMR timescale, not investigated but likely involving the pyramidal rotation of the $M(CO)_n$ fragment to render time-averaged equivalence for all CO ligands in the fragment.

Table 3. Selected IR[a] and $^{31}P\{^1H\}$ NMR Data[b] for New Compounds

Compound	ν(CO)	δ_P (J_{PP}) [J_{PW}]		
		PCy_2	P	PMe
$[Mo_2FeCp_2(\mu_3\text{-}P)(\mu\text{-}PCy_2)(\mu_3\text{-}PMe)(CO)_5]$ (**2a**)	2010 (vs), 1945 (m), 1927 (m), 1892 (m)	151.4 (14, 9)	239.2 (9)	268.2 (14)
$[Mo_2WCp_2(\mu_3\text{-}P)(\mu\text{-}PCy_2)(\mu_3\text{-}PMe)(CO)_6]$ (**2d**)	2010 (vs), 1911 (vs)	165.7 (br)	124.5 (br)	321.5 (br)
$[MnMo_2Cp_2Cp'(\mu\text{-}PCy_2)(\mu_3\text{-}P_2Me)(CO)_4]$ (**3b**)		157.4 (br)[c]	–42.9 (br, 400)[c]	–180.3 (br, 400)[c]
$[Mo_2WCp_2(\mu\text{-}PCy_2)(\mu_3\text{-}P_2Me)(CO)_7]$ (**3d**)	2065 (w), 1938 (vs), 1918 (m, sh)[d]	148.7 (56, 16)[e]	–236.7 (419, 56)[e]	–154.9 (419, 16)[e]
$[MnMo_2Cp_2Cp'(\mu_3\text{-}P)(\mu\text{-}PCy_2)(CO)_4]$ (**4b**)	1941 (s), 1885 (vs)	117.6	1103.3	
$[Mo_3Cp_2(\mu_3\text{-}P)(\mu\text{-}PCy_2)(CO)_7]$ (**4c**)	2064 (m), 1947 (vs)	124.7	1159.3	
$[Mo_2WCp_2(\mu_3\text{-}P)(\mu\text{-}PCy_2)(CO)_7]$ (**4d**)	2062 (m), 1942 (vs)	126.8	1081.4 [156]	
$[MnMo_2Cp_2Cp'(\mu_3\text{-}P)(\mu\text{-}PCy_2)(CO)_5]$ (**5**)	1964 (s), 1924 (vs), 1889 (s), 1859 (s)	223.2 (11)	951.0 (11)	
$[Mo_2WCp_2(\mu_3\text{-}P)(\mu\text{-}PCy_2)(\mu\text{-}CO)(CO)_5]$ (**6**)	2063 (m), 1941 (vs), 1714 (w)	246.0 (30)	925.2 (30) [160]	

[a] Recorded in dichloromethane solution, with C–O stretching bands [ν(CO)] in cm^{-1}. [b] Recorded in CD_2Cl_2 at 121.50 MHz and 298 K, with coupling constants (J_{PP}) and [J_{PW}] in Hz. [c] In tetrahydrofuran at 162.14 MHz. [d] In toluene. [e] In toluene at 162.14 MHz.

Incorporation of 16-Electron Metal Fragments. Reactions of **1** with the metal carbonyl adducts $[MnCp'(CO)_2(THF)]$ and $[W(CO)_5(THF)]$ at room temperature yielded the expected trinuclear complexes $[MnMo_2Cp_2Cp'(\mu\text{-}PCy_2)(\mu_3\text{-}\kappa^2\text{:}\kappa^2\text{:}\kappa^1\text{-}P_2Me)(CO)_4]$ (**3b**) and $[Mo_2WCp_2(\mu\text{-}PCy_2)(\mu_3\text{-}\kappa^2\text{:}\kappa^2\text{:}\kappa^1\text{-}P_2Me)(CO)_7]$ (**3d**) following from addition of the corresponding 16-electron metal fragments *via* the LP of the apical P atom of the diphosphenyl ligand (Scheme 2; Cp' = η^5-C_5H_4Me). However, these compounds turned out to be rather unstable and could only be characterized partially in solution by IR and NMR inspection of the crude reaction mixtures, which progressively evolve to give the corresponding phosphide complexes $[MnMo_2Cp_2Cp'(\mu_3\text{-}P)(\mu\text{-}PCy_2)(CO)_4]$ (**4b**) and $[Mo_2WCp_2(\mu_3\text{-}P)(\mu\text{-}PCy_2)(CO)_7]$ (**4d**). The tungsten compound **3d** was thermally more robust, and full transformation into **4d** was more conveniently completed upon stirring a toluene solution of the complex at 343 K for 2 h. However, we noticed that both transformations **3a,d**/**4a,d** occur very rapidly upon attempted chromatographic purification on alumina even at 253 K. We finally note that compounds **4** follow from formal loss of methylphosphinidene in the diphosphenyl complexes **3**, but the fate of this unstable molecule could not be determined, since no major resonances other than those attributed to compounds **4b** and **4d** were present in the ^{31}P NMR spectra of the corresponding reaction mixtures.

Reaction of compound **1** with the related THF adduct $[Mo(CO)_5(THF)]$ is more complex, since it gives initially three different products that we have only identified through the ^{31}P NMR spectra of the crude reaction mixture. These uncharacterized substances (denoted as **A**, **B** and **C**, see the experimental section) decompose rapidly during attempted purification, to give the phosphide derivative $[Mo_3Cp_2(\mu_3\text{-}P)(\mu\text{-}PCy_2)(CO)_7]$ (**4c**) as the unique product. Since the latter is isolated in good yield after chromatographic workup (ca. 75%), we suggest that all three species eventually

decompose to give the same phosphide derivative **4c**. Although we have not characterized these intermediates, it is obvious that they still preserve the PMe moiety, because they all display three distinct ^{31}P NMR resonances. However, the connectivity between the P atoms of the former diphosphenyl ligand could not be unambiguously determined in compounds **A** to **C**, since they all exhibit moderate P–P couplings in the range 80-100 Hz, thus ruling out a type **G** coordination of this ligand comparable to that observed in compounds **3**, characterized by one-bond couplings much larger (ca. 400 Hz). In any case, our results indicate that the κ^2:κ^2:κ^1-coordination mode of the diphosphenyl ligand in these systems (type **G** in Chart 1) is somehow disfavored, a matter to be discussed later on.

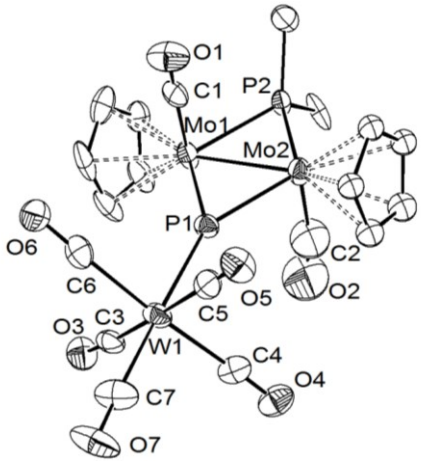

Figure 3. ORTEP diagram (30% probability) of compound **4d** with H atoms and Cy groups (except the C^1 atoms) omitted for clarity.

Table 4. Selected Bond Lengths (Å) and Angles (°) for Compound **4d**

Mo1–Mo2	2.749(2)	P2–Mo1–P1	107.8(1)
Mo1–P1	2.305(4)	P2–Mo2–P1	109.0(1)
Mo2–P1	2.302(4)	Mo1–P1–Mo2	73.3(1)
Mo1–P2	2.417(3)	Mo1–P2–Mo2	69.9(1)
Mo2–P2	2.383(3)	C1–Mo1–Mo2	79.1(5)
P1–W1	2.457(3)	C2–Mo2–Mo1	84.6(8)
Mo1–C1	2.04(2)	Mo1–P1–W1	144.4(2)
Mo2–C2	2.00(2)	Mo2–P1–W1	142.4(2)
W1–C3	2.01(2)	P1–W1–C3	90.5(4)
W1–C4	2.03(2)	P1–W1–C4	87.1(5)
W1–C5	2.06(2)	P1–W1–C5	89.6(4)
W1–C6	2.06(2)	P1–W1–C6	87.1(5)
W1–C7	2.03(2)	P1–W1–C7	178.1(7)

Solid-State and Electronic Structure of 4d. The structure of this phosphide-bridged complex was confirmed through a single-crystal X-ray diffraction analysis (Figure 3 and Table 4). Although there is some disorder reducing the quality of data (see the Experimental Section) the essential structural features are well defined. The molecule is built from two MoCp(CO) fragments arranged in a transoid fashion and symmetrically bridged by a PCy_2 ligand and by a trigonal planar phosphide ligand (P1), which is also

bound to an exocyclic $W(CO)_5$ moiety, thus completing an octahedral coordination environment around the W atom. The Mo atoms are likely connected through a double bond, as suggested by the short intermetallic separation of 2.749(2) Å, which is only marginally longer than the one determined for the related 32-electron diphenylphosphide complex $[Mo_2Cp_2(\mu\text{-}PPh_2)_2(CO)_2]$ (ca. 2.71 Å).[24] As found for the latter molecule, the planar Mo_2P_2 core is nearly perpendicular to the average plane defined by the Mo atoms and the carbonyl ligands attached to them (C1–Mo1–Mo2–P1 ca. 88º), while the latter ligands are leaning over the Mo–Mo vector (Mo–Mo–CO ca. 80º). These structural features are characteristic of all unsaturated complexes of the type $[Mo_2Cp_2(\mu\text{-}PCy_2)(\mu\text{-}X)(CO)_2]$ previously described by us (X = H, R, CR, COR, NCHR).[25]

Analysis of the binding in the planar trigonal (Σ(M–P1–M´) ca. 360º) phosphide ligand of **4d** is less straightforward. There are some ten complexes with this geometry around phosphorus structurally characterized so far. Among them, those involving Mo or W atoms display quite diverse M–P lengths, in the range 2.27-2.54 Å, obviously following from accommodation of the phosphide ligand to different electronic demands of the metal fragments bound to it. In the case of **4d**, the Mo–P lengths of ca. 2.30 Å are ca. 0.1 Å shorter than the corresponding lengths for the PCy_2 ligand, and therefore indicative of substantial multiplicity in these bonds. Actually, these lengths are almost identical to those measured for the phosphinidene-bridged complexes $[Mo_2Cp_2(\mu\text{-}PMes^*)(CO)_4]$,[26] $[Mo_2Cp_2I_2(\mu\text{-}PMes^*)(CO)_2]$,[27] and $[Mo_2Cp_2(\mu\text{-}PMes^*)(\mu\text{-}CO)_2]$,[28] which also display planar trigonal environments around the P atom, with formal Mo–P bond orders of 1.5,[29,30] while the formal intermetallic bond orders increase from 1 to 3 along this series. The W1–P1 distance of 2.457(3) Å in **4d** can be considered as consistent with a description of the corresponding interaction as a dative P→W bond. The obvious metric reference in this case are mononuclear phosphine compounds of type $[W(CO)_5(PR_3)]$, but an inspection of the (many) available structures in the Cambridge Crystallographic database revealed that these distances are considerably influenced by the steric demands of the R groups. In the absence of strong steric repulsions these W–P lengths are usually found slightly below 2.50 Å, reaching values as short as 2.45 Å for some cyclic phosphines,[31] or even ca. 2.38 Å for cyclic phosphites.[32]

The above geometric analysis supports our view of the P–W interaction in **4d** as a dative single bond, while π bonding of the phosphide ligand would mainly involve the Mo atoms. A similar situation has been previously found in the alkoxide complexes $[W_4(OR)_4(\mu_3\text{-}P)_2(CO)_{10}]$ (R = Xyl, ^{t}Bu), with P–W lengths of ca. 2.29 Å and P→$W(CO)_5$ lengths of ca. 2.50 Å.[33] However, in the cluster $[W_3(C_5H_4{}^t\text{Bu})_3(\mu_3\text{-}P)(CO)_7]$ the W–P lengths are comparable to the above ones,[34] even if the long P–W bond now

involves a 17-electron $W(CO)_3Cp$ fragment. In order to further clarify the π(P–M) interactions in our complexes we carried out density functional theory (DFT) calculations on **4d** and analyzed the corresponding molecular orbitals (see the Supporting Information), as well as the electron density in the M–M and M–P bonds, as managed under the atoms in molecules (AIM) framework.[35]

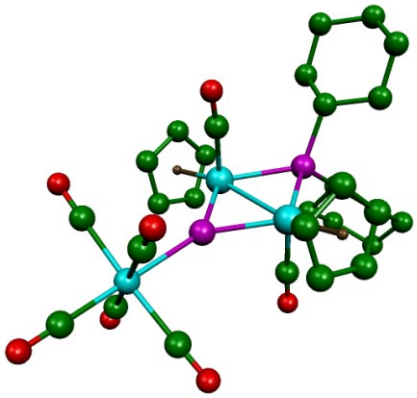

Figure 4. DFT-Optimized structure of compound **4d** with H atoms omitted for clarity. Selected bond lengths (Å): Mo–Mo = 2.797; Mo–PCy_2 = 2.456, 2.448; Mo–P = 2.335, 2.330; W–P = 2.516.

The DFT-optimized geometry of **4d** (Figure 4) is in good agreement with the structure determined crystallographically, with computed distances involving the metal atoms a bit longer than the experimental figures, as usually found in this sort of calculations. Bonding at the central Mo_2P_2 core is strongly reminiscent of that one computed for the 32-electron carbyne complex $[Mo_2Cp_2(\mu\text{-}CCO_2Me)(\mu\text{-}PCy_2)(CO)_2]$ at the same level of theory.[25c] The Mo–Mo double bond in **4d** follows from a configuration of the type $\delta^2\sigma^2\pi^2\delta^{*2}$, with the δ^* orbital (HOMO–1, MO166) involved in backbonding to the carbonyls, while the δ orbital (MO159) is strongly stabilized through mixing with the p_π orbital of the phosphide ligand, thus accounting for the π(P–Mo) interaction within the Mo_2P ring (Figure 5). We note that the latter orbital also contains some contribution of the W atom, thus pointing to some involvement of the latter in π-bonding with the phosphide ligand, but the extent of this interaction is difficult to quantify from a simple orbital analysis. To further clarify this point we then examined the electron densities (ρ) at the bond critical points (bcp) of the bonds of interest (Table 5). First we noticed that the electron density at the Mo–Mo bcp (0.394 eÅ^{-3}) is only slightly lower than the value computed for the mentioned carbyne complex (0.444 eÅ^{-3}), substantially higher than the values of ca. 0.2 eÅ^{-3} computed for single Mo–Mo bonds in related species,[25c] and therefore consistent with the double intermetallic bond formulated for this molecule. As for the bonds involving the phosphide ligand, we note that electron density at the Mo–P bpcs (ca. 0.65 eÅ^{-3}) is substantially higher than those at the strong single bonds of the PCy_2 ligand (ca. 0.53 eÅ^{-3}), somewhat higher than the value of ca. 0.59 eÅ^{-3} computed for the more congested phosphinidene-bridged complex $[Mo_2Cp_2(\mu\text{-}PMes^*)(\mu\text{-}CO)_2]$ (with a formal Mo–P bond order of 1.5) and nearly identical to the figure of 0.654 eÅ^{-3}

computed for the double Mo–P bond in [$Mo_2Cp_2(\mu$-PH)$(CO)_2(\eta^6$-HMes*)].[36] All of this is indicative of a strong π interaction between the phosphide ligand and the Mo atoms. In contrast, the electron density at the W–P bpc (0.439 eÅ^{-3}) is even lower than those involving the PCy_2 ligand, and therefore points to a single bond interaction with negligible π contribution from the phosphide ligand. In fact, the electron density computed for an hypothetical $WP(CO)_5$ molecule with the W–P fixed length of 2.516 Å (the value in the optimized structure of **4d**) is not lower, but slightly higher (0.492 eÅ^{-3}), surely due to increased backbonding from the tungsten-based orbitals. Moreover, we note that electron distribution within the Mo_2P ring is little perturbed upon removal of the full $W(CO)_5$ fragment to yield a molecule with a bent μ_2-P ligand [$Mo_2Cp_2(\mu_2$-P)$(\mu$-$PCy_2)(CO)_2$] (**4d-W**) (see the Supporting Information). Indeed the electron density at the Mo–P bcps in **4d-W** (0.67 eÅ^{-3}, Table 5) is only marginally higher than that in **4b**, this further indicating that the π interaction of the tungsten atom with the phosphide ligand in **4b** is negligible.

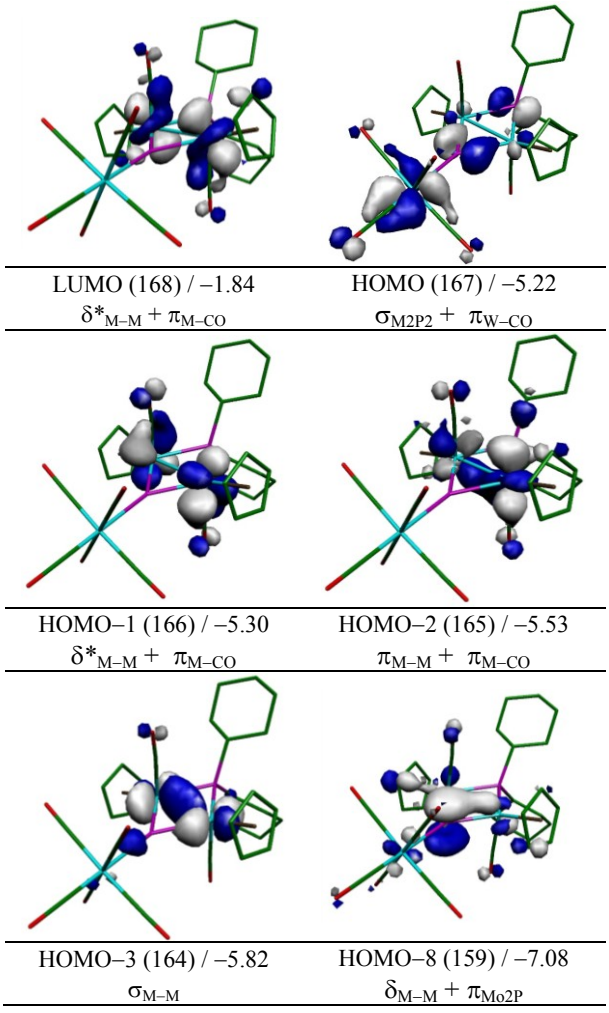

Figure 5. Selected molecular orbitals computed for **4d**, with their energies (in eV) and main bonding character indicated below.

Table 5. Topological Properties of the Electron Density at the Bond Critical Points.[a]

Bond	4d		4d–W		5[b]	
	ρ	$\nabla^2\rho$	ρ	$\nabla^2\rho$	ρ	$\nabla^2\rho$
Mo1–Mo2	0.394	0.923	0.419	1.046	Not located	
Mo1–P	0.653	2.851	0.668	2.260	0.731	3.371
Mo2–P	0.658	2.836	0.672	2.252	0.370	1.403
W/Mn–P	0.439	3.623			0.628	4.039
Mo1–PCy	0.524	3.018	0.519	3.156	0.551	3.346
Mo2–PCy	0.534	2.976	0.527	3.113	0.398	2.160

[a] Values of the electron density at the bond critical points (ρ) are given in eÅ^{-3}, and those of its Laplacian at these points ($\nabla^2\rho$) are given in eÅ^{-5}. [b] Mo2 refers to the atom bearing two CO ligands.

In summary, from the precedent analysis we conclude that π interaction of the phosphide ligand in **4d** is essentially located over the Mo_2P triangle, much in the same way as the π interaction of a bridging carbyne ligand, whereas its interaction with the W atom is best described as just a single donor P→W bond. Thus we can think of the P→$W(CO)_5$ fragment as an isolobal analogue of a carbyne ligand (CR). Indeed the frontier orbitals of such phosphide fragment (see the Supporting Information) are alike those of a carbyne,[37,38] and such analogy will be useful to guide and interpret the reactivity of compounds **4** to be discussed later on.

Solution Structure of Compounds 3 and 4. As mentioned earlier, the diphosphenyl complexes **3b,d** could only be partially characterized in solution by IR and ^{31}P NMR inspection of the crude reaction mixtures, due to their low stability (Table 3). Unambiguous assignment of the C–O stretches of **3b** could not be done, while the IR spectrum of **3d** was dominated by bands attributed to its $W(CO)_5$ fragment (2065 (w), 1938 (vs) and 1918 (m, sh) cm^{-1}). Their ^{31}P{^{1}H} NMR spectra display three different resonances in each case, with the most deshielded one (δ_P ca. 150 ppm) being assigned to the PCy_2 ligand by analogy with the parent methyldiphosphenyl complex and related compounds.[1] The diphosphenyl ligand gives rise to two upfield doublets in each case, displaying a large J_{PP} value above 400 Hz which is indicative of direct P–P bonding, and individual assignment of these resonances in **3d** to the PMe (δ_P −154.9 ppm) and P (δ_P −236.7 ppm) atoms could be unambiguously made by comparison of ^{1}H-decoupled and undecoupled spectra. Assignment of the broad resonances observed for the manganese compound **3b** was made on the assumption that, compared to **3d**, the P resonance should be largely shifted downfield, because of the change in metal (Mn vs. W), this leading to its identification with the −42.9 ppm resonance. Indeed we have shown previously that resonances of heterometal-bound P atoms in diphosphorus-bridged complexes $[Mo_2MCp_2(\mu\text{-}\kappa^2\text{:}\kappa^2\text{:}\kappa^1\text{-}P_2)(\mu\text{-}PCy_2)(CO)_2L_n]$ move upfield by some 100 ppm as we go from 1st- to 2nd-row metals, and by a similar amount when moving from 2nd- to 3rd-row metals.[1b]

Spectroscopic data in solution for compounds **4** are consistent with the solid-state structure of **4d**. Once more, bands due to the $Mo_2(CO)_2$ oscillator were not appreciated in the solution IR spectra for these complexes, which instead were dominated by the bands arising from the ML_n fragments terminally bound to the phosphide ligand ($MnCp'(CO)_2$ and $M(CO)_5$). Yet, the ^1H and $^{13}C\{^1H\}$ NMR spectra of these compounds are as expected for molecules with a C_2 axis containing both P nuclei, thus rendering CO, Cp and Cy pairs equivalent in the Mo_2 unit. The most remarkable spectroscopic feature of compounds **4**, however, is found in their $^{31}P\{^1H\}$ NMR spectra, which in each case display two negligibly coupled resonances, as typically found for mixed PR_2 complexes of the type *trans*-$[M_2Cp_2(\mu\text{-}PR_2)(\mu\text{-}PR'_2)(CO)_2]$ also having planar M_2P_2 cores.[39] The PCy_2 group in compounds **4** give rise to a resonance at ca. 120 ppm, a position comparable to those found in the mentioned mixed complexes. In contrast, the phosphide ligand gives rise to a dramatically deshielded resonance at around 1100 ppm, which is characteristic of planar trigonal phosphide ligands coordinated to three metal centers. Yet, this shift still is substantially higher than those measured for related phosphide-bridged complexes involving similar metal atoms (cf. 885 ppm for $[W_2Re_2Cp^*_2(\mu_3\text{-}P)_2(CO)_{12}]$,[7] 882.5 ppm for $[MoW_2Cp(\mu_3\text{-}P)(CO)_{12}]$,[14] or even 558.2 ppm for $[W_4(OXyl)_4(\mu_3\text{-}P)_2(CO)_{10}]$).[33a]

Reaction Pathways to the Trinuclear Derivatives of 1. In spite of the diverse output of the reactions of **1** with different metal carbonyl solvates discussed so far, these all seem to be initiated analogously, then evolving differently depending on the nature of each particular metal fragment being added (Scheme 3). The first step in all cases would be the incorporation of a 16-electron metal fragment ML_n ($Fe(CO)_4$, $W(CO)_4(THF)$, $MnCp'(CO)_2$, $Mo(CO)_5$, $W(CO)_5$) to the P atom bearing the lone pair in the diphosphenyl ligand, to yield $\kappa^2{:}\kappa^2{:}\kappa^1$-diphosphenyl intermediates **F** only detected in some cases (**3b,d**). When the added fragment is $W(CO)_4(THF)$, this first step would be naturally followed by THF dissociation and insertion of the resulting unsaturated $W(CO)_4$ fragment in the P–P bond of the diphosphenyl ligand and creation of a new W–Mo bond, to eventually give the phosphide phosphinidene complex **2d**. Formation of the iron product **2a** likely would proceed analogously from the corresponding intermediate of type **G**, after spontaneous decarbonylation of the $Fe(CO)_4$ fragment. Interestingly, the first step in the suggested sequence leading to compounds **2** is related to the electrophilic activation of P_4 by silylenes, phosphenium cations and related carbene-like species,[40] a process also resulting in the eventual insertion of the added electrophile in a P–P bond. In contrast, intermediates of type **G** not releasing easily a ligand from the ML_n fragment (as it is the case of fragments $MnCp'(CO)_2$ and $W(CO)_5$) would alternatively evolve through extrusion of the phosphinidene "PMe" moiety to give compounds **4**. It is difficult to identify the origin of the low stability of type **G**

intermediates in these reactions, but the steric pressure introduced by the relatively bulky ML_n fragments being added might by a major factor contributing to this effect. The case of the $Mo(CO)_5$ fragment stands apart, since three different intermediates, none of them with a structure of type **G**, seems to precede the formation of corresponding phosphide derivative **4c**, as noted above, and we will not speculate about their possible nature.

Scheme 3

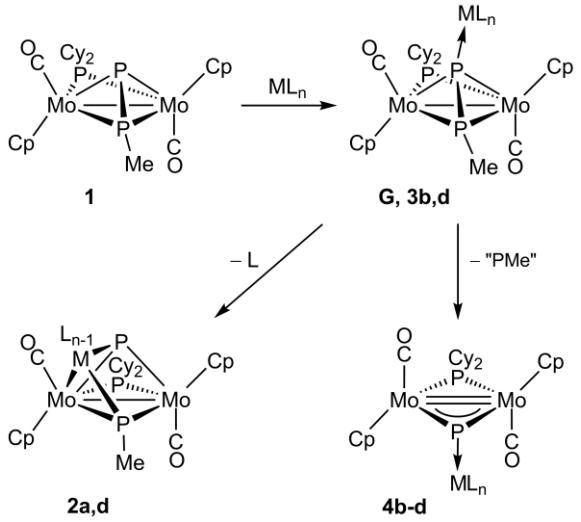

Carbon Monoxide Uptake and Release in Phosphide-Bridged Complexes 4. We have shown above that, at the structural and electronic level, the phosphide-bridged complexes **4** can be related to carbyne complexes of the type $[Mo_2Cp_2(\mu\text{-}CX)(\mu\text{-}PCy_2)(CO)_2]$ by virtue of the isolobal relationship between $PW(CO)_5$ and CX moieties, and we might ask whether this analogy can be also extended to their chemical behavior. As a proof of concept to address this question, we have examined carbonylation and decarbonylation reactions of some of these phosphide complexes.

The 32-electron carbyne complexes mentioned above have been shown to be carbonylated to give either ketenyl $[Mo_2Cp_2\{\mu\text{-}C(X)CO\}(\mu\text{-}PCy_2)(CO)_2]$ or tricarbonyl $[Mo_2Cp_2(\mu\text{-}CX)(\mu\text{-}PCy_2)(CO)_3]$ derivatives, depending on X (OMe, Ph).[25c,b] The manganese complex **4b** readily reacts with CO under mild conditions (293 K, 3 bar) to give the pentacarbonyl derivative $[MnMo_2Cp_2Cp'(\mu_3\text{-}P)(\mu\text{-}PCy_2)(CO)_5]$ (**5**), an electron-precise molecule following from coordination of a CO molecule and *trans* to *cis* rearrangement of the Mo_2Cp_2 moiety (Scheme 4). This reaction thus matches exactly the carbonylation of the methoxycarbyne complex $[Mo_2Cp_2(\mu\text{-}COMe)(\mu\text{-}PCy_2)(CO)_2]$, including the *trans* to *cis* rearrangement, a behavior also shown by some other isoelectronic species such as the alkenyl complexes $[Mo_2Cp_2(\mu\text{-}\eta^1\text{:}\eta^2\text{-}CHCHR)(\mu\text{-}PCy_2)(CO)_2]$ (R = H, *p*-tolyl),[41] and even by the diethylphosphide complex $[Mo_2Cp_2(\mu\text{-}PEt_2)_2(CO)_2]$.[39] We note that compound **5** is a rather unstable molecule that starts to release carbon monoxide when removing the CO atmosphere, to regenerate the parent

compound **4b**. Yet, we were able to grow a few crystals of it, thus enabling its full structural characterization, to be discussed below.

Scheme 4

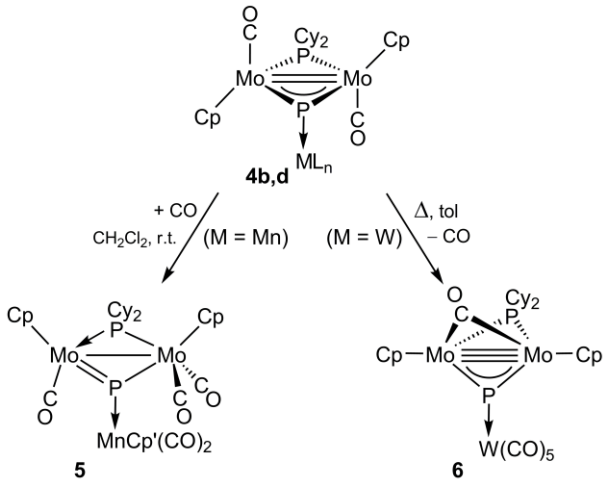

On the other hand, we have shown previously that the carbyne complexes $[Mo_2Cp_2(\mu\text{-}CX)(\mu\text{-}PCy_2)(CO)_2]$ usually require photochemical activation in order to remove a CO molecule out of them, although the benzylidyne complex (X = Ph) can be decarbonylated very slowly in refluxing toluene solutions.[25b,c] In all cases, however, the product formed is the corresponding 30-electron monocarbonyl $[Mo_2Cp_2(\mu\text{-}CX)(\mu\text{-}PCy_2)(\mu\text{-}CO)]$ with a Mo–Mo triple bond.[42] In a similar way, the tungsten complex **4d** was decarbonylated in refluxing toluene solution to give $[Mo_2WCp_2(\mu_3\text{-}P)(\mu\text{-}PCy_2)(\mu\text{-}CO)(CO)_5]$ (**6**), a molecule retaining an intact $PW(CO)_5$ fragment bound to an unsaturated dimolybdenum center now formally bearing an intermetallic triple bond (Scheme 4).

Solid-State and Solution Structure of 5. The molecule of **5** in the crystal is built from MoCp(CO) and $MoCp(CO)_2$ fragments directly bonded to each other and displaying a cisoid arrangement of the Cp ligands (Figure 6 and Table 6). These two fragments are bridged by a PCy_2 ligand and by a trigonal planar phosphide ligand (P2), which is also coordinated to an exocyclic $MnCp'(CO)_2$ fragment. The corresponding Mn–P distance of 2.153(2) Å is comparable to the value measured for the phosphite complex $[Mn(\eta^5\text{-triindane})(CO)_2\{P(OMe)_3\}]$ (2.1673(6) Å),[43] and therefore consistent with the formulation of a single dative bond for this interaction, as found for **4d**. The Mo–Mo distance of 3.1318(7) Å is consistent with a single Mo–Mo bond as predicted under the 18-electron formalism while using the isolobal relationship discussed above, which implies a 3-electron contribution of the $P\rightarrow MnCp'(CO)_2$ fragment to the dimetal unit, and is only marginally longer than those measured for related species such as the alkenyl complex $[Mo_2Cp_2(\mu\text{-}\eta^1\text{:}\eta^2\text{-}CHCH_2)(\mu\text{-}PCy_2)(CO)_3]$ (3.0858(7) Å),[41a] but ca. 0.34 Å longer than the figure of 2.749(2) Å measured for the Mo–Mo double bond in **4d**. The P atoms bridging the Mo_2 unit define a puckered PMo_2P rhombus

(P1–Mo2–Mo1–P2 ca. 132°) with distances to Mo1 substantially shorter than those to Mo2, thus balancing the lower coordination number of the former atom. The Mo1–PCy_2 length of 2.385(1) Å is ca. 0.15 Å shorter than the Mo2–PCy_2 one (2.551(2) Å), therefore consistent with formal P→Mo1 and P–Mo2 descriptions for these bonds. As for the phosphide ligand, the Mo1–P and Mo2–P lengths (2.233(2) and 2.577(1) Å) are respectively shorter and much longer than the average value of ca. 2.30 Å measured for the symmetrical phosphide ligand in **4d**, thus supporting the formulation of double and single Mo–P bonds, respectively (Scheme 3).[36] The phosphide asymmetry in **5** is thus more pronounced than those found for the complexes $[Cr_2WCp(\mu_3\text{-}P)(CO)_{12}]$,[44] and $[MoW_2(\mu_3\text{-}P)Cp(CO)_{12}]$,[14] which display short M–P lengths of ca. 2.26 and 2.30 Å respectively.

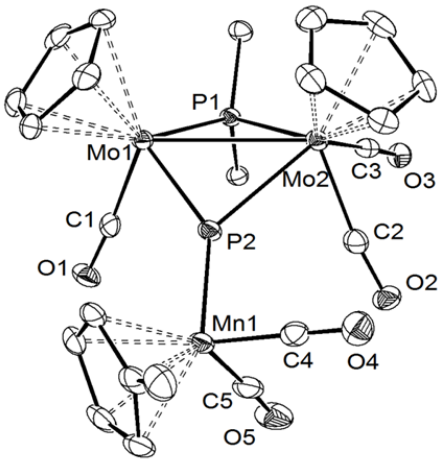

Figure 6. ORTEP diagram (30% probability) of compound **5** with H atoms and Cy groups (except the C^1 atoms) omitted for clarity.

Table 6. Selected Bond Lengths (Å) and Angles (º) for Compound **5**.

Mo1–Mo2	3.1318(7)	P2–Mo1–P1	94.95(5)
Mo1–P1	2.385(1)	P2–Mo2–P1	83.22(5)
Mo2–P1	2.551(2)	Mo1–P1–Mo2	78.69(5)
Mo1–P2	2.233(2)	Mo1–P2–Mo2	80.91(5)
Mo2–P2	2.577(1)	Mo1–P2–Mn1	143.21(8)
P2–Mn1	2.153(2)	Mo2–P2–Mn1	135.82(8)
Mo1–C1	1.942(6)	C1–Mo1–Mo2	111.5(2)
Mo2–C2	1.933(6)	C2–Mo2–Mo1	111.3(2)
Mo2–C3	1.961(6)	C3–Mo2–Mo1	116.6(2)
Mn1–C4	1.784(7)	C2–Mo2–C3	76.5(2)
Mn1–C5	1.787(7)	C4–Mn1–C5	91.5(3)

To further support our description of the phosphide bonding in **5** we carried out DFT calculations analogous to those discussed for **4d** (see the Supporting Information). The optimized structure is comparable to the one determined crystallographically, with the phosphide ligand bridging the Mo atoms very asymmetrically (Mo–P = 2.251, 2.678 Å). The molecular orbitals in this case are heavily mixed and therefore little informative in this respect, but the electron density at the Mo1–P bond critical point (0.731 $eÅ^{-3}$, Table

5) is substantially higher than the value of ca. 0.65 eÅ^{-3} for the symmetrical phosphide in **4d** and nearly doubles the figure for the long Mo2–P bond (0.370 eÅ^{-3}), all of this being consistent with the formulations of double and single Mo–P bonds respectively.

Spectroscopic data in solution for **5** are in good agreement with its solid-state structure. Its IR spectrum displays four rather than the five C–O stretches expected from the superimposition of bands arising from independent $Mo_2(CO)_3$ and $Mn(CO)_2$ oscillators, surely as a result of accidental degeneracy of two of them. Its $^{31}P\{^1H\}$ NMR spectrum displays the characteristic strongly deshielded resonance corresponding to the trigonal planar phosphide (δ_P 951.0 ppm), which now is visibly coupled ($^2J_{PP}$ =11 Hz) to the PCy_2 resonance (δ_P 223.2 ppm), thus reflecting the reduced P–Mo–P angle in this molecule (average 89^o), when compared to **4d** (ca. 109^o).[45] We note that the PCy_2 resonance in **5** is 100 ppm higher than that in the precursor **4b**. This is a general trend found when comparing related couples of complexes with formal double and single Mo-Mo bonds, such as $[Mo_2Cp_2(\mu\text{-}PEt_2)_2(CO)_n]$ (δ_P 78.7 and 194.7 ppm for n = 2 and 3),[39] $[Mo_2Cp_2(\mu\text{-}\eta^1\text{:}\eta^2\text{-}CHCH_2)(\mu\text{-}PCy_2)(CO)_n]$ (δ_P 135.0 and 250.5 ppm for n = 2 and 3),[41] or $[Mo_2Cp_2(\mu\text{-}COMe)(\mu\text{-}PCy_2)(CO)_n]$ (δ_P 125.0 and 219.7 ppm for n = 2 and 3).[25c]

Solution Structure of 6. Although crystals suitable for an X-ray analysis could not be obtained for this compound, spectroscopic data in solution are enough to define its structure (Scheme 4). Its IR spectrum exhibits two bands at high frequencies (2063 (m) and 1941 (vs) cm^{-1}) corresponding to the $W(CO)_5$ fragment, and a weaker band at low frequency (1714 cm^{-1}) characteristic of a bridging CO ligand, also identified through its strongly deshielded ^{13}C NMR resonance (δ_C 296.8 ppm). The $^{31}P\{^1H\}$ NMR spectrum of **6** displays the expected highly deshielded resonance corresponding to the μ_3-P ligand (δ_P 925.2 ppm), which is also appreciably coupled ($^2J_{PP}$ =30 Hz) to the PCy_2 resonance (δ_P 246.0 ppm). Indeed, $^2J_{PP}$ couplings in the related triply-bonded monocarbonyls $[Mo_2Cp_2(\mu\text{-}PR_2)(\mu\text{-}PR'R'')(\mu\text{-}CO)]$ fall in the range 20-30 Hz, and their ^{31}P chemical shifts also are very high (cf. 263.7 ppm for $[Mo_2Cp_2(\mu\text{-}PCy_2)_2(\mu\text{-}CO)]$).[39] The ^1H and $^{13}C\{^1H\}$ spectra are indicative of a structure having a symmetry plane containing the P atoms bridging the Mo_2 unit, thus rendering the Cp ligands equivalent. Yet, the Cy groups remain inequivalent, as indicated by the presence of eight resonances (four per group) in the $^{13}C\{^1H\}$ spectrum. Again, fast rotation on the NMR timescale around the P–W bond renders the equatorial CO ligands of the $W(CO)_5$ fragment equivalent, as denoted by the presence of a single resonance corresponding to these four ligands (197.5 ppm) and a separated one for the axial carbonyl (206.4 ppm), in a 4 to 1 intensity ratio.

Conclusions

The methyldiphosphenyl complex **1** easily incorporates 16-electron ML_n fragments to give unstable trinuclear diphosphenyl complexes $[Mo_2MCp_2(\mu\text{-}PCy_2)(\mu_3\text{-}\kappa^2\text{:}\kappa^2\text{:}\kappa^1\text{-}P_2Me)(CO)_2L_n]$ evolving *via* two main pathways: (a) release of an L ligand (L = THF, CO) with concomitant P–P bond cleavage and formation of a new Mo–M bond, to give phosphide- and phosphinidene-bridged derivatives of type $[Mo_2MCp_2(\mu_3\text{-}P)(\mu\text{-}PCy_2)(\mu_3\text{-}PMe)L_{n-1}]$; (b) release of methylphosphinidene (PMe), to give the corresponding phosphide-bridged derivatives $[Mo_2MCp_2(\mu_3\text{-}P)(\mu\text{-}PCy_2)(CO)_2L_n]$. The latter display planar trigonal phosphide ligands involved in strong π bonding with the unsaturated Mo_2 center of these molecules, while the M–P interaction with the exocyclic ML_n fragment can be described as a single dative bond, a view further supported by DFT calculations, which also allow us to identify an isolobal analogy between the $P\rightarrow ML_n$ fragments in these products and a carbyne ligand (CR). The latter analogy enables in turn an easy interpretation and prediction of the reactivity of these unsaturated complexes concerning their uptake and release of simple ligands as carbon monoxide, which reproduces the chemical behavior of carbyne-bridged complexes $[Mo_2Cp_2(\mu\text{-}CX)(\mu\text{-}PCy_2)(CO)_2]$ and related molecules.

Experimental Section

General Procedures and Starting Materials. All manipulations and reactions were carried out under a nitrogen (99.995%) atmosphere using standard Schlenk techniques. Solvents were purified according to literature procedures, and distilled prior to use.[46] All reagents were obtained from the usual commercial suppliers and used as received, unless otherwise stated, except for compounds $[MnCp'(CO)_2(THF)]$,[47] $[M(CO)_5(THF)]$ (M = Mo, W),[48] and $[Mo_2Cp_2(\mu\text{-}PCy_2)(\mu\text{-}\kappa^2\text{:}\kappa^2\text{-}P_2Me)(CO_2)]$ (**1**),[1] which were prepared as described previously. Photochemical experiments were performed using jacketed Pyrex Schlenk tubes, cooled by tap water (ca. 288 K). A 400 W mercury lamp placed ca. 1 cm away from the Schlenk tube was used for these experiments. Modified literature procedures were employed in the preparation of adducts $[M(CO)_4(THF)_2]$ (M= Mo, W);[49] the Mo complex was obtained at 288 K at low reaction times, whereas formation of the W complex required longer reaction times (1.5-2 h) and lower temperatures (273 K). In both cases, IR monitoring was used to determine the optimum reaction time. Petroleum ether refers to that fraction distilling in the range 338-343 K. Chromatographic separations were carried out using jacketed columns refrigerated by tap water or by a closed 2-propanol circuit kept at the desired temperature with a cryostat. Commercial aluminum oxide (activity I, 150 mesh) was degassed under vacuum prior to use. The latter was mixed under nitrogen with the appropriate amount of water to reach activity IV. IR stretching frequencies of CO ligands were measured in solution (using CaF_2 windows), or in Nujol mulls, are referred to as ν(CO) and are

given in wave numbers (cm^{-1}). Nuclear magnetic resonance (NMR) spectra were routinely recorded at 300.13 (^1H), 121.50 ($^{31}P\{^1H\}$) or 75.47 MHz ($^{13}C\{^1H\}$) at 298 K in CD_2Cl_2 solution unless otherwise stated. Chemical shifts (δ) are given in ppm, relative to internal tetramethylsilane (^1H, ^{13}C) or external 85% aqueous H_3PO_4 solutions (^{31}P). Coupling constants (J) are given in Hertz.

Preparation of [$Mo_2FeCp_2(\mu_3$-P)(μ-PCy_2)(μ_3-PMe)$(CO)_5$] (2a). Solid [$Fe_2(CO)_9$] (0.025 g, 0.070 mmol) was added to a solution of compound **1** (0.045 g, 0.069 mmol) in dichloromethane (5 mL), and the mixture was stirred for 1 h at room temperature to give a brown-orange solution mainly containing compound **2a**, along with smaller amounts of a tetranuclear derivative. Solvent was then removed under vacuum, the residue was extracted with dichloromethane/petroleum ether (1/9) and the extracts were chromatographed through alumina at 288 K. An orange fraction was eluted with the same solvent mixture which gave, after removal of solvents, compound **2a** as an orange microcrystalline solid (0.020 g, 36%). Crystals suitable for an X-ray analysis were grown by slow diffusion of a layer of petroleum ether into a concentrated toluene solution of the complex at 253 K. Anal. Calcd for $C_{28}H_{35}FeMo_2O_5P_3$: C, 42.45; H, 4.45. Found: C, 42.58; H, 4.64. ν(CO)(Nujol): 2010 (s), 1950 (s), 1936 (s), 1903 (vs), 1868 (m), 1829 (w, sh). ^1H NMR: δ 5.34 (d, J_{PH} = 1, 5H, Cp), 5.22 (s, 5H, Cp), 2.37 (d, J_{PH} = 8, 3H, PMe), 1.90-1.10 (m, 22H, Cy). $^{31}P\{^1H\}$ NMR: δ 268.2 (d, J_{PP} = 14, μ_3-PMe), 239.2 (d, J_{PP} = 9, μ_3-P), 151.4 (dd, J_{PP} = 14, 9, μ-PCy_2). ^{31}P NMR: δ 268.2 (m, br, μ_3-PMe), 239.2 (d, br, J_{PP} = 9, μ_3-P), 151.4 (m, μ-PCy_2). $^{13}C\{^1H\}$ NMR: δ 236.9 (s, br, MoCO), 229.1 (d, J_{CP} = 40, MoCO), 212.8 (s, 3FeCO), 88.0, 87.9 (2s, Cp), 52.2 [dd, J_{CP} = 9, 2, C^1(Cy)], 43.8 [dd, J_{CP} = 11, 11, C^1(Cy)], 37.5 [s, C^2(Cy)], 36.1 [s, $2C^2$(Cy)], 34.3 [d, J_{CP} = 5, C^2(Cy)], 29.6 (d, J_{CP} = 47, PMe), 28.9 [d, J_{CP} = 11, C^3(Cy)], 28.3 [d, J_{CP} = 10, $2C^3$(Cy)], 28.2 [d, J_{CP} = 8, C^3(Cy)], 26.4, 26.2 [2s, C^4(Cy)].

Preparation of [$Mo_2WCp_2(\mu_3$-P)(μ-PCy_2)(μ_3-PMe)$(CO)_6$] (2d). A tetrahydrofuran solution (5 mL) of the adduct [$W(CO)_4(THF)_2$], prepared *in situ* from [$W(CO)_6$] (0.017 g, 0.048 mmol), was added to a tetrahydrofuran solution (5 mL) of compound **1** (0.030 g, 0.046 mmol), and the mixture was stirred for 50 min to give a brown-orange solution containing compounds **2d** and **3d** in a ratio of ca. 5:2, along with small amounts of **4d**. Solvent was then removed under vacuum, the residue was extracted with dichloromethane/petroleum ether (1/8) and the extracts were chromatographed through alumina at 288 K. Elution with dichloromethane/petroleum ether (1/5) gave a brown-grey fraction yielding, after removal of solvents, compound **2d** as a brown solid (0.027 g, 62%). The crystals used in the X-ray study were grown by the slow diffusion of a layer of petroleum ether into a concentrated dichloromethane solution of the complex at 253 K. Anal. Calcd for $C_{29}H_{35}Mo_2O_6P_3W$: C, 36.73; H, 3.72. Found: C, 37.46; H, 3.69. ^1H NMR: δ 5.39 (s, br, 5H, Cp), 5.24 (d, J_{PH} = 1, 5H, Cp), 2.21 (m, 1H, Cy), 1.95 (d,

J_{PH} = 5, 3H, PMe), 1.90-1.10 (m, 21H, Cy). $^{31}P\{^1H\}$ NMR: δ 321.5 (s, br, μ_3-PMe), 165.7 (s, br, μ-PCy_2), 124.5 (s, br, μ_3-P). $^{13}C\{^1H\}$ NMR: δ 215.9 (s, WCO), 91.1, 88.6 (2s, Cp), 51.4 [dd, J_{CP} = 7, 5, C^1(Cy)], 37.8 [s, C^2(Cy)], 36.7 [s, $2C^2$(Cy)], 36.4 [dd, J_{CP} = 6, 4, C^1(Cy)], 34.0 [d, J_{CP} = 5, C^2(Cy)], 29.2 [d, J_{CP} = 11, C^3(Cy)], 29.2 [d, J_{CP} = 43, PMe], 28.7, 28.6 [2d, J_{CP} = 11, C^3(Cy)], 28.3 [d, J_{CP} = 8, C^3(Cy)], 26.6 [s, br, $2C^4$(Cy)]; the resonances corresponding to the Mo-bound CO ligands could not be clearly identified in this spectrum.

Preparation of solutions of [$MnMo_2Cp_2Cp'(\mu$-$PCy_2)(\mu_3$-κ^2:κ^2:κ^1-$P_2Me)(CO)_4$] (3b). A tetrahydrofuran solution (5 mL) of the adduct [MnCp'$(CO)_2$(THF)], prepared *in situ* from [MnCp'$(CO)_3$] (6 μL, 0.038 mmol), was added to a tetrahydrofuran solution (5 mL) of compound **1** (0.020 g, 0.031 mmol), and the mixture was stirred at room temperature for 40 min to give a brown-orange solution containing compound **3b** as major product, along with small amounts of a tetranuclear compound. These species are both very unstable and decompose upon manipulation to give compound **4b** as the only carbonyl-containing product. $^{31}P\{^1H\}$ NMR (tetrahydrofuran, 162.14 MHz): δ 157.4 (s, br, μ-PCy_2), –42.9 (d, br, J_{PP} = 400, PMn), –180.3 (d, br, J_{PP} = 400, PMe).

Preparation of solutions of [$Mo_2WCp_2(\mu$-$PCy_2)(\mu_3$-κ^2:κ^2:κ^1-$P_2Me)(CO)_7$] (3d). A tetrahydrofuran solution (5 mL) of the adduct [$W(CO)_5$(THF)], prepared *in situ* from [$W(CO)_6$] (0.011 g, 0.031 mmol), was added to a tetrahydrofuran solution (5 mL) of compound **1** (0.020 g, 0.031 mmol), and the mixture was stirred for 1 h in a Schlenk tube equipped with a Young's valve to give a brown-orange solution containing compound **3d** as the major species. Attempts to further purify this compound were unsuccessful due to its progressive decomposition to give the phosphide complex **4d**. $^{31}P\{^1H\}$ NMR (toluene, 162.14 MHz): δ 148.7 (dd, J_{PP} = 56, 16, μ-PCy_2), –154.9 (dd, J_{PP} = 419, 16, PMe), –236.7 (dd, J_{PP} = 419, 56, PW). ^{31}P NMR (toluene, 162.14 MHz): δ 148.7 (d, br, J_{PP} = 56, μ-PCy_2), –154.9 (d, br, J_{PP} = 419, PMe), –236.7 (dd, J_{PP} = 419, 56, PW).

Preparation of [$MnMo_2Cp_2Cp'(\mu_3$-P)(μ-$PCy_2)(CO)_4$] (4b). A tetrahydrofuran solution (5 mL) of compound **1** (0.030 g, 0.046 mmol) was added to a tetrahydrofuran solution of the adduct [MnCp'$(CO)_2$(THF)], prepared *in situ* from [MnCp'$(CO)_3$] (28 μL, 0.178 mmol), and the mixture was stirred at room temperature for 90 min to give a brown-orange solution containing a mixture of **4b** and **3b** in a ratio of ca. 1:1, along with small amounts of a tetranuclear complex. Solvent was then removed, the residue was extracted with dichloromethane/petroleum ether (1:6) and the extracts were chromatographed through alumina at 253 K. Elution with dichloromethane/petroleum ether (1:8) gave first an orange fraction which was discarded, and then a yellow one yielding, after removal of solvents, compound **4b** as an orange solid (0.026 g, 71%). Anal. Calcd for $C_{32}H_{39}MnMo_2O_4P_2$: C, 48.26; H, 4.94. Found: C, 48.03; H, 4.98. ^1H

NMR: δ 5.76 (s, 10H, Cp), 5.15 (m, 2H, C_5H_4), 4.96, 4.94 (2m, 2 x 1H, C_5H_4), 2.45 (m, 2H, Cy), 2.02 (s, 3H, Me), 2.0-1.0 (m, 20H, Cy). $^{31}P\{^1H\}$ NMR: δ 1103.3 (s, μ_3-P), 117.6 (s, μ-PCy_2). $^{31}P\{^1H\}$ NMR (161.98 MHz, 223 K): δ 1094.4 (s, μ_3-P), 116.3 (s, μ-PCy_2). $^{13}C\{^1H\}$ NMR (100.61 MHz, 223 K): δ 231.9 (s, br, MoCO), 222.9 (s, br, MnCO), 90.6 (s, Cp), 102.6 [s, $C^1(C_5H_4)$], 86.4, 85.5, 85.1, 83.7 [4s, $CH(C_5H_4)$], 43.7 [d, J_{CP} = 20, C^1(Cy)], 35.5 [s, C^2(Cy)], 30.3 [s, C^2(Cy)], 28.1 [d, J_{CP} = 12, C^3(Cy)], 28.0 [s, J_{CP} = 12, C^3(Cy)], 26.3 [s, br, C^4(Cy)], 14.2 (s, Me).

Preparation of [$Mo_3Cp_2(\mu_3$-P)(μ-PCy_2)$(CO)_7$] (4c). A tetrahydrofuran solution (5 mL) of the adduct [$Mo(CO)_5$(THF)], prepared *in situ* from [$Mo(CO)_6$] (0.010 g, 0.038 mmol), was added to a tetrahydrofuran solution (5 mL) of compound **1** (0.020 g, 0.031 mmol), and the mixture was stirred for 1 h to give a brown solution containing three unidentified products (**A**, **B** and **C**) in similar amounts. Solvent was then removed under vacuum, the residue was extracted with dichloromethane/petroleum ether (1/3) and the extract was chromatographed through alumina at 253 K. Elution with the same solvent mixture gave a yellow fraction yielding, after removal of solvents, compound **4c** as a yellow solid (0.020 g, 76%). Anal. Calcd for $C_{29}H_{32}Mo_3O_7P_2$ (**4c**): C, 41.35; H, 3.83. Found: C, 41.70; H, 3.81. *Spectroscopic data for compound **4c***: ^1H NMR: δ 5.86 (s, 10H, Cp), 2.50 (m, 2H, Cy), 2.10-1.00 (m, 20H, Cy). *Spectroscopic data for compound **A***: $^{31}P\{^1H\}$ NMR (tetrahydrofuran): δ 299.6 (dd, J_{PP} = 93, 17, μ-P), 138.6 (dd, J_{PP} = 16, 8, μ-PCy_2), 137.9 (dd, J_{PP} = 93, 8, μ-P). *Spectroscopic data for compound **B***: $^{31}P\{^1H\}$ NMR (tetrahydrofuran): δ 144.6 (dd, J_{PP} = 83, 51, μ-PCy_2), 115.8 (dd, J_{PP} = 146, 83, μ-P), 27.2 (dd, J_{PP} = 146, 51, μ-P). *Spectroscopic data for compound **C***: $^{31}P\{^1H\}$ NMR (tetrahydrofuran): δ 262.9 (dd, J_{PP} = 85, 13, μ-P), 155.9 (dd, J_{PP} = 13, 6, μ-PCy_2), 153.0 (dd, J_{PP} = 85, 6, μ-P).

Preparation of [$Mo_2WCp_2(\mu_3$-P)(μ-PCy_2)$(CO)_7$] (4d). A tetrahydrofuran solution (5 mL) of the adduct [$W(CO)_5$(THF)], prepared *in situ* from [$W(CO)_6$] (0.011 g, 0.031 mmol), was added to a tetrahydrofuran solution (5 mL) of compound **1** (0.020 g, 0.031 mmol) and the mixture was stirred for 50 min. The solvent was then removed under vacuum, the residue dissolved in toluene (7 mL), and the solution stirred for 2 h at 343 K to give an orange solution containing **4d** as major species. Solvent was then removed under vacuum, the residue extracted with dichloromethane/petroleum ether (1/4) and the extract chromatographed through alumina at 288 K. Elution with the same solvent mixture gave a yellow fraction yielding, after removal of solvents, compound **4d** as a yellow solid (0.020 g, 69%). Crystals suitable for X-ray diffraction analysis were obtained by the slow diffusion of a layer of petroleum ether into a concentrated toluene solution of the complex at 253 K. Anal. Calcd for $C_{29}H_{32}Mo_2O_7P_2W$: C, 37.44; H, 3.47. Found: C, 37.11; H, 3.42. ^1H NMR: δ 5.86 (s, 10H, Cp), 2.49 (d, br, J_{PH} = 13, 2H, Cy), 2.09 (m, 2H, Cy), 2.0-1.0 (m, 18H, Cy). $^{13}C\{^1H\}$ NMR (100.61 MHz): δ 218.1 (t, J_{CP} =

12, MoCO), 212.6 [d, J_{CP} = 15, WCO(ax)], 198.5 [d, J_{CP} = 3, WCO(eq)], 91.5 (s, Cp), 45.6 [d, J_{CP} = 2, C^1(Cy)], 35.8 [d, J_{CP} = 2, C^2(Cy)], 33.5 [s, C^2(Cy)], 28.27 [d, J_{CP} = 11, C^3(Cy)], 28.26 [d, J_{CP} = 13, C^3(Cy)], 26.4 [s, C^4(Cy)].

Preparation of [$MnMo_2Cp_2Cp'(\mu_3$-P)(μ-PCy_2)$(CO)_5$] (5). A dichloromethane solution (4 mL) of compound **4b** (0.020 g, 0.025 mmol) was placed in a bulb equipped with a Young's valve. The bulb was cooled at 77 K, evacuated under vacuum, and then refilled with CO. The valve was then closed, and the solution was allowed to reach room temperature and further stirred for 10 min to give an orange solution mainly containing compound **5**, which was obtained as a red-orange solid upon removal of solvent. This compound undergoes spontaneous decarbonylation to give back compound **4b** in the absence of a CO atmosphere and therefore it was not isolated as a pure solid in bulk. However, a few crystals of **5** suitable for an X-ray analysis were grown by the slow diffusion of layers of petroleum ether and diethyl ether into a concentrated toluene solution of the complex (contaminated with **4b**) at 253 K. ν(CO)(Nujol): 1963 (m, sh), 1953 (s), 1910 (m), 1902 (m, sh), 1894 (vs), 1847 (s). ^{1}H NMR: δ 5.28, 5.19 (2s, 2 x 5H, Cp), 4.79 (m, 2H, C_5H_4), 4.67, 4.63 (2m, 2 x 1H, C_5H_4), 1.96 (s, 3H, Me), 2.50-0.80 (m, 22H, Cy). ^{1}H NMR (400.13 MHz, 223 K): δ 5.30, 5.22 (2s, 2 x 5H, Cp), 4.85 (m, 2H, C_5H_4), 4.72, 4.61 (2m, 2 x 1H, C_5H_4), 1.97 (s, 3H, Me), 2.50-0.80 (m, 22H, Cy). ^{31}P{^{1}H} NMR: δ 951.0 (d, J_{PP} = 11, μ_3-P), 223.2 (s, J_{PP} = 11, μ-PCy_2). ^{31}P{^{1}H} NMR (161.98 MHz, 223 K): δ 942.6 (s, μ_3-P), 220.9 (s, μ-PCy_2). ^{13}C{^{1}H} NMR (100.61 MHz, 223 K): δ 93.5, 89.9 (2s, Cp), 86.8, 86.1, 85.8, 83.5 [4s, CH(C_5H_4)], 36.7 [d, J_{CP} = 15, C^1(Cy)], 35.4, 34.0, 33.6 [3s, C^2(Cy)], 28.9 [d, J_{CP} = 10, C^3(Cy)], 28.5 [d, J_{CP} = 9, C^3(Cy)], 27.7 [s, C^2(Cy)], 27.5, 27.4 [2d, J_{CP} = 15, C^3(Cy)], 26.6, 26.2 [2s, C^4(Cy)], 14.2 (s, Me). Resonances due to carbonyl ligands and the C1 atom of the C_5H_4 ring could not be identified in this spectrum, whereas the missing C^1(Cy) resonance most likely is obscured by that of the solvent.

Preparation of [$Mo_2WCp_2(\mu_3$-P)(μ-PCy_2)(μ-CO)$(CO)_5$] (6). A tetrahydrofuran solution (7 mL) of compound **1** (0.030 g, 0.046 mmol) was mixed with a tetrahydrofuran solution of [$W(CO)_5$(THF)], prepared *in situ* from 0.017 g (0.048 mmol) of [$W(CO)_6$], in a Schlenk tube equipped with a Young's valve, and the mixture was stirred for 50 min at room temperature to give a brown-orange solution. Solvent was then removed under vacuum and the residue was dissolved in toluene (7 mL) and refluxed for 3 h. After removal of solvent, the residue was extracted with dichloromethane/petroleum ether (1/2) and the extract chromatographed through alumina. Elution with dichloromethane/petroleum ether (1/5) gave first a yellow fraction containing small amounts of **4d** and then an orange fraction yielding, after removal of solvents, compound **6** as a red solid (0.023 g, 55%). Anal. Calcd for $C_{28}H_{32}Mo_2O_6P_2W$: C, 37.28; H, 3.58. Found: C, 37.20; H, 3.56. ^{1}H NMR: δ 5.95 (s,

10H, Cp), 1.95-0.90 (m, 18H, Cy), 0.59, 0.45 (2m, 2 x 2H, Cy). $^{31}P\{^1H\}$ NMR: δ 925.2 (d, J_{PP} = 30, J_{PW} = 160, μ_3-P), 246.0 (d, J_{PP} = 30, μ-PCy_2). $^{13}C\{^1H\}$ NMR (150.91 MHz): δ 296.8 (s, μ-CO), 206.4 [d, J_{CP} = 17, WCO(ax)], 197.5 [d, J_{CP} = 6, J_{CW} = 127, WCO(eq)], 94.1 (s, Cp), 44.6 [d, J_{CP} = 16, C^1(Cy)], 40.8 [d, J_{CP} = 19, C^1(Cy)], 33.7, 33.1 [2s, C^2(Cy)], 27.6, 27.3 [2d, J_{CP} = 12, C^3(Cy)], 26.3, 25.9 [2s, C^4(Cy)].

X-Ray Structure Determination for Compounds 2a, 2d, 4d and 5. Data collection for these compounds was performed on an Oxford Diffraction Xcalibur Nova single crystal diffractometer, using Cu-Kα radiation (λ= 1.5418 Å) at 100 K (**2a**) or 123 K. Images were collected at a 90 mm (**2a**) or 63 mm fixed crystal-detector distance, using the oscillation method, with 1º oscillation and variable exposure time per image (11-16 s for **2a**, 1.5-2 s for **2d**, 5-80 s for **4d** and 25-60 s for **5**). Data collection strategy was calculated with the program CrysAlis Pro CCD.[50] Data reduction and cell refinement was performed with the program CrysAlis Pro RED.[50] An empirical absorption correction was applied using the SCALE3 ABSPACK algorithm as implemented in the program CrysAlis Pro RED. Using the program suite WinGX,[51] the structures were generally solved by Patterson interpretation and phase expansion using SHELXL97,[52] and refined with full-matrix least squares on F^2 using SHELXL97, except for **2d**, solved with SIR92.[53] In general all the positional parameters and the anisotropic temperature factors of all non-H atoms were refined anisotropically, except for the carbon atoms involved in disorder, which were refined isotropically to prevent their temperature factors from becoming non-positive definite, and all hydrogen atoms were geometrically placed and refined using a riding model. Compound **2a** crystallized with a molecule of toluene, found to be disordered and placed on a symmetry element. This disorder could not be solved, therefore the SQUEEZE procedure,[54] as implemented in PLATON,[55] was used. Upon squeeze application and convergence the strongest residual peak (0.94 e A^{-3}) was placed between the Mo(2) and P(1) atoms. In the case of **2d** there were two independent molecules of the complex and a molecule of dichloromethane in the asymmetric unit. One of the cyclopentadienyl ligands in each case was disordered over two positions, and satisfactorily modeled with occupancies 0.5/0.5 and 0.6/0.4 respectively. In the case of **4d**, one of the carbonyl ligands and one of the cyclopentadienyl groups also were disordered. The cyclopentadienyl group was satisfactorily modeled over two positions with 0.5/0.5 occupancy. However, the disorder in the C(2)O(2) ligand could not be solved; moreover, the corresponding thermal ellipsoids had no chemical sense, so eventually these atoms were refined isotropically with restraints in the Mo(2)–C(2) and C(2)–O(2) distances to get a sensible

geometry for this CO group, analogous to that of the other Mo-bound carbonyl. Crystallographic data and structure refinement details for all these compounds are collected in Table 7.

Table 7. Crystal Data for New Compounds

	2a	**2d**·1/2CH_2Cl_2	**4d**	**5**
mol formula	$C_{28}H_{35}FeMo_2O_5P_3$	$C_{59}H_{72}Cl_2Mo_4O_{12}P_6W_2$	$C_{29}H_{32}Mo_2O_7P_2W$	$C_{33}H_{39}MnMo_2O_5P_2$
mol wt	792.20	1981.35	930.22	824.4
cryst syst	monoclinic	triclinic	triclinic	monoclinic
space group	$P\,2_1/c$	$P\,\bar{1}$	$P\,\bar{1}$	$P\,2_1/c$
radiation (λ, Å)	1.54184	1.54184	1.54184	1.54184
a, Å	9.9099(2)	11.458(5)	10.4478(8)	10.9898(3)
b, Å	23.5511(5)	18.270(5)	11.2943(12)	15.1118(4)
c, Å	15.7915(4)	18.747(5)	14.2992(17)	19.6212(9)
α, deg	90	111.258(5)	71.451(11)	90
β, deg	116.591(2)	99.502(5)	88.166(8)	100.840(4)
γ, deg	90	106.801(5)	83.909(8)	90
V, Å^3	3295.7(1)	3337.3(19)	1590.6(3)	3200.5(2)
Z	4	2	2	4
calcd density, g cm^{-3}	1.597	1.972	1.942	1.711
absorp coeff, mm^{-1}	11.275	14.728	14.21	10.757
temperature, K	100(2)	124(3)	123(2)	123(2)
θ range (deg)	8.81 to 69.60	2.81 to 74.55	3.26 to 74.83	3.72 to 69.34
index ranges (h, k, l)	–11, 11; –28, 28; –19, 18	–14, 14; –22, 22; –23, 23	–12, 9; –13, 13; –16, 17	–13, 13; –13, 17; –23, 22
no. of reflns collected	17884	60753	12329	14021
no. of indep reflns (R_{int})	6059 (0.0296)	13398 (0.0451)	6180 (0.0951)	5857 (0.0546)
reflns with $I > 2\sigma(I)$	5408	11684	3627	4604
R indexes [data with $I > 2\sigma(I)$][a]	R_1 = 0.0303 wR_2 = 0.0863[b]	R_1 = 0.0328 wR_2 = 0.0802[c]	R_1 = 0.0695 wR_2 = 0.1673[d]	R_1 = 0.0523 wR_2 = 0.1292[e]
R indexes (all data)[a]	R_1 = 0.0345 wR_2 = 0.0888[b]	R_1 = 0.0399 wR_2 = 0.0855[c]	R_1 = 0.1221 wR_2 = 0.2121[d]	R_1 = 0.0686 wR_2 = 0.1424[e]
GOF	1.074	1.045	0.954	1.013
no. of restraints/params	0 / 353	0 / 758	12 / 354	0 / 389
$\Delta\rho$(max., min.), eÅ^{-3}	0.941, –0.654	1.279, –1.428	1.520, –1.689	2.546, –1.488

[a] $R = \Sigma||F_o| - |F_c|| / \Sigma|F_o|$. $wR = [\Sigma w(|F_o|^2 - |F_c|^2)^2 / \Sigma w|F_o|^2]^{1/2}$. $w = 1/[\sigma^2(F_o^2) + (aP)^2 + bP]$ where $P = (F_o^2 + 2F_c^2)/3$. [b] a = 0.0504, b = 2.6898. . [c] a = 0.0403, b = 8.5689. [d] a = 0.0899, b = 0.0000. [e] a = 0.0841, b = 0.0000.

Computational Details. Computations were carried out using the GAUSSIAN03 package,[56] in which the hybrid methods B3LYP and UB3LYP ($PW(CO)_5$) were applied with the Becke three parameters exchange functional[57] and the Lee-Yang-Parr correlation functional.[58] An accurate numerical integration grid (99,590) was used for all the calculations via the keyword Int=Ultrafine. Effective core potentials (ECP) and their associated double-ζ LANL2DZ basis set were used for the metal atoms.[59] The light elements (P, O, C and H) were described with 6-31G* basis set.[60] Geometry optimizations were performed under no symmetry restrictions, using initial coordinates derived from the X-ray data of **4d** and **5**. Frequency analyses were performed for all

stationary points to ensure that a minimum structure with no imaginary frequencies was achieved in each case. Molecular orbitals were visualized using the MOLEKEL program,[61] and the topological analysis of the electron density was carried out with the *Xaim* routine.[62]

Supporting Information Available. A CIF file containing full crystallographic data for compounds **2a**, **2d**, **4d** and **5** (CCDC 1013089 to 1013092) and a pdf file containing details of DFT calculations of compounds **4d**, **5** and related fragments (atomic coordinates, selected bond lengths and angles, and molecular orbitals). This material is available free of charge via the Internet at http://pubs.acs.org.

Author Information. Corresponding authors: *E-mail: ara_12_79@hotmail.com (A.R.), mara@uniovi.es (M.A.R).

Acknowledgment. We thank the DGI of Spain for financial support (Projects CTQ2009-09444 and CTQ2012-33187) and the CMC of the Universidad de Oviedo for access to computing facilities. A. R. thanks the Spanish Research Council for Scientific Research (CSIC) for a JAE-Doc contract, co-funded by the European Social Fund (ESF).

References

1. (a) Alvarez, M. A.; García, M. E.; García-Vivó, D.; Ramos, A.; Ruiz, M. A. *Inorg. Chem.* **2011**, *50*, 2064. (b) Alvarez, M. A.; García, M. E.; García-Vivó, D.; Ramos, A.; Ruiz, M. A. *Inorg. Chem.* **2012**, *51*, 11061.
2. Weber, L. *Chem. Rev.* **1992**, *82,* 1839.
3. (a) Weber, L.; Meine, G.; Boese, R.; Bläser, D. *Chem. Ber.* **1988**, *121*, 853. (b) Weber, L.; Meine, G. *Chem. Ber.* **1987**, *120*, 457.
4. (a) Weber, L.; Schumann, I.; Stammler, H.-G.; Neumann, B. *J. Organomet. Chem.* **1993**, *443*, 175. (b) A similar coordination mode is displayed at the phosphine-diphosphorus-bridged CoPt complex $[CoPt(\mu\text{-}P_2PPh_2CH_2PPh_2)_2(PPh_3)_2]BF_4$. See: Caporalli, M.; Barbaro, P.; Gonsalvi, L.; Ienco, A.; Yakhvarov, D.; Peruzzini, M. *Angew. Chem., Int. Ed.* **2008**, *47*, 3766.
5. Feske, D.; Queisser, J.; Schottmüller, H. *Z. Anorg. Allg. Chem.* **1996**, *622*, 1731.
6. Weber, L.; Schumann, H. *Chem. Ber.* **1991***, 124*, 265.
7. Scherer, O. J.; Ehses, M.; Wolmershäuser, G. *Angew. Chem. Int. Ed.* **1998**, *37*, 507.
8. (a) Caporali, M.; Gonsalvi, L.; Rossin, A.; Peruzzini, M. *Chem. Rev.* **2010**, *110*, 4178. (b) Cossairt, B. M.; Piro, N. A.; Cummins, C. C. *Chem. Rev.* **2010**, *110*, 4164.

9. Alvarez, M. A.; García, M. E.; Lozano, R.; Ramos, A.; Ruiz, M. A., results to be published.
10. Alvarez, M. A.; García, M. E.; García-Vivó, D.; Lozano, R.; Ramos, A.; Ruiz, M. A. *Inorg. Chem.* **2013**, *52*, 9005.
11. Alvarez, C. M.; Alvarez, M. A.; García, M. E.; Ramos, A.; Ruiz, M. A.; Graiff, C.; Tiripicchio, A. *Organometallics* **2007**, *26*, 321.
12. Cordero, B.; Gómez, V.; Platero-Prats, A. E.; Revés, M.; Echeverría, J.; Cremades, E.; Barragán, F.; Alvarez, S. *Dalton Trans.* **2008**, 2832.
13. Scheer, M.; Leiner, E.; Kramkowski, P.; Schiffer, M.; Baum, G. *Chem. Eur. J.* **1998**, *4*, 1917.
14. Scheer, M.; Himmel, D.; Kuntz, C.; Zhan, S.; Leiner, E. *Chem. Eur. J.* **2008**, *14*, 9020.
15. (a) Cotton, F. A.; Frenz, B. A.; White, A. J. *Inorg. Chem*. **1974**, *13*, 1407. (b) Klasen, C.; Lorenz, I. P.; Schmid, S.; Beuter, G. *J. Organomet. Chem*. **1992**, *428*, 363. (c) Alvarez, C. M.; Galán, B.; García, M. E.; Riera, V.; Ruiz, M. A.; Vaissermann, J. *Organometallics* **2003**, *22*, 5504. (d) Alvarez, M. A.; García, M. E.; García-Vivó, D.; Ramos, A.; Ruiz, M. A. *Inorg. Chem.* **2012**, *51*, 3698.
16. Alvarez, C. M.; Alvarez, M. A.; García, M. E.; González, R.; Ramos, A.; Ruiz, M. A. *Inorg. Chem.* **2011**, *50*, 10937.
17. Bridgeman, A. J.; Mays, M. J.; Woods, A. D. *Organometallics* **2001**, *20*, 2076.
18. Braterman, P. S. *Metal Carbonyl Spectra*; Academic Press: London, U. K., 1975.
19. (a) García, M. E.; García-Vivó, D.; Ruiz, M. A. *Organometallics* **2009**, *28*, 4385. (b) Alvarez, M. A.; García, M. E.; Martínez, M. E.; Ruiz, M. A. *Organometallics* **2010**, *29*, 904.
20. Mays, M. J.; Raithby, P. R.; Sarveswaran, K.; Solan, G. A. *Dalton Trans.* **2002**, 1671.
21. Huttner, G.; Knoll, K. *Angew. Chem., Int. Ed. Engl.* **1987**, *26*, 743.
22. Carty, A. J.; MacLaughlin, S. A.; Nucciarone, D. in *Phosphorus-31 NMR Spectroscopy in Stereochemical Analysis;* Verkade, J. G., Quin, L. D., Eds.; VCH: Deerfield Beach, FL, 1987; Chapter 16.
23. Davies, J. E.; Klunduk, M. C.; Mays, M. J.; Raithby, P. R.; Shields, G. P.; Tompkin, P. K. *J. Chem. Soc., Dalton Trans.* **1997**, 715.
24. Adatia, T.; McPartlin, M.; Mays, M. J.; Morris, M. J.; Raithby, P. R. *J. Chem. Soc. Dalton Trans.* **1989**, 1555.
25. (a) García, M. E.; Ramos, A.; Ruiz, M. A.; Lanfranchi, M.; Marchiò, L. *Organometallics* **2007**, *26*, 6197. (b) Alvarez, M. A.; García, M. E.; García-Vivó, D.; Martínez, M. E.; Ruiz, M. A. *Organometallics* **2011**, *30*, 2189. (c) García, M. E.; García-Vivó, D.; Ruiz, M. A.; Alvarez, S.; Aullón, G. *Organometallics* **2007**,

26, 5912. (d) Alvarez, M. A.; García, M. E.; Ramos, A.; Ruiz, M. A. *Organometallics* **2007**, *26*, 1461.

26. Arif, A. M.; Cowley, A. H.; Norman, N. C.; Orpen, A. G.; Pakulski, M. *Organometallics* **1988**, *7*, 309.
27. García, M. E.; Riera, V.; Ruiz, M. A.; Sáez, D.; Vaissermann, J.; Jeffery, J. C. *J. Am. Chem. Soc*. **2002**, *124*, 14304.
28. Amor, I.; García, M. E.; Ruiz, M. A.; Sáez, D.; Hamidov, H.; Jeffery, J. C. *Organometallics* **2006**, *25*, 4857.
29. Huttner, G.; Evertz, K. *Acc. Chem. Res.* **1986**, *19*, 406.
30. Alvarez, M. A.; Amor, I.; García, M. E.; García-Vivó, D.; Ruiz, M. A.; Hamidov, H.; Jeffery, J. C. *Inorg. Chim. Acta* **2014**, in press (DOI: http://dx.doi.org/10.1016/j.ica.2014.04.043).
31. Bode, M.; Schnakenburg, G.; Daniels, J.; Marinetti, A.; Streubel, R. *Organometallics* **2010**, *29*, 656.
32. Ulbaev, T. S.; Mardashev, Y. S.; Koroteev, M. P.; Khrustalev, V. N.; Antipin, M. Y. *Zh. Strukt. Khim.* **2005**, *4*6, 924.
33. (a) Kramkowski, P.; Baum, G.; Radius, U.; Kaupp, M.; Scheer, M. *Chem. Eur. J.* **1999**, *5*, 2890. (b) Scheer, M.; Kramkowski, P.; Schuster, K. *Organometallics* **1999**, *18*, 2874.
34. Groer, T.; Scheer, M. *Z. Anorg. Allg. Chem.* **2000**, *626*, 1211.
35. Bader, R. F. W. *Atoms in molecules-A Quantum Theory*; Oxford University Press: Oxford, U. K., 1990.
36. Alvarez, M. A.; Amor, I.; García, M. E.; García-Vivó, D.; Ruiz, M. A.; Suárez, J. *Organometallics* **2010**, *29*, 4384.
37. (a) Hoffmann, R. *Angew. Chem., Int. Ed. Engl.* **1982**, *21*, 711. (b) Stone, F. G. A. *Angew. Chem., Int. Ed. Engl.* **1984**, *23*, 89.
38. Jean, Y. *Molecular Orbitals of Transition Metal Complexes*; Oxford University Press: Oxford, U. K., 2003, Chapter 5.
39. García, M. E.; Riera, V.; Ruiz, M. A.; Rueda, M. T.; Sáez, D. *Organometallics* **2002**, *21*, 5515.
40. (a) Giffin, N. A.; Masuda, J. D. *Coord. Chem. Rev.* **2011**, *255*, 1342. (b) Scheer, M.; Balazs, G.; Seitz, A. *Chem. Rev.* **2010**, *110*, 4236.
41. (a) Alvarez, M. A.; García, M. E.; Ramos, A.; Ruiz, M. A. *J. Organomet. Chem.* **2009**, *694*, 3864. (b) Alvarez, M. A.; García, M. E.; Ramos, A.; Ruiz, M. A.; Lanfranchi, M.; Tiripicchio, A. *Organometallics* **2007**, *26*, 5454.
42. (a) García, M. E.; García-Vivó, D.; Ruiz, M. A.; Alvarez, S.; Aullón, G. *Organometallics* **2007**, *26*, 4930. (b) Alvarez, M. A.; García, M. E.; García-Vivó, D.; Menéndez, S.; Ruiz, M. A. *Organometallics* **2013**, *32*, 218.

43. Reginato, N.; McGlinchey, M. J. *Organometallics* **2001**, *20*, 4147.
44. Huttner, G.; Weber, U.; Sigwarth, B.; Scheidsteger, O.; Lang, H.; Zsolnai L. *J. Organomet. Chem.* **1985**, *282*, 331.
45. A general trend established for $^2J_{XY}$ in complexes of the type [MCpXYL$_2$] is that it increases algebraically with the XMY angle, with absolute values in the order $|J_{cis}| > |J_{trans}|$. See, for instance, Jameson, C. J. In *Phosphorus-31 NMR Spectroscopy in Stereochemical Analysis*; Verkade, J. G., Quin, L. D., Eds.; VCH: Deerfield Beach, FL, 1987; Chapter 6.
46. Armarego, W. L. F.; Chai, C. *Purification of Laboratory Chemicals*, *5th Edition*; Butterworth-Heinemann: Oxford, UK, 2003.
47. Johnson, E. C.; Meyer, T. J.; Winterton, N. *Inorg. Chem.* **1971**, *10*, 218.
48. Hermann, W. W. *Angew. Chem.* **1974**, *86*, 345.
49. (a) Gibson, V. C.; Long, N. J.; Long, R. J.; White, A. J. P.; Williams, C. K.; Williams, D. J.; Grigiotti, E.; Zanello, P. *Organometallics* **2004**, *23*, 957. (b) Sellman, D.; Brandl, A.; Endell, R. *J. Organomet. Chem.* **1975**, *97*, 229.
50. *CrysAlis Pro*; Oxford Diffraction Ltd.: Oxford, U. K., 2006.
51. Farrugia, L. J. *J. Appl. Crystallogr.* **1999**, *32*, 837.
52. Sheldrick, G. M. *Acta Crystallogr.* **2008**, *A64*, 112.
53. Altomare, A.; Cascarano, G.; Giacovazzo, C.; Guagliardi, A.; Burla, M. C.; Polidori, G.; Camalli, M. *J. Appl. Crystallogr.* **1994**, *27*, 435.
54. Van der Sluis, P.; Spek, A. L. *Acta Crystallogr.* **1990**, *A46*, 194.
55. Spek, A. L. *PLATON, A Multipurpose Crystallographic Tool*; Utrecht University: Utrecht, The Netherlands, 2010.
56. Frisch, M. J.; Trucks, G. W.; Schlegel, H. B.; Scuseria, G. E.; Robb, M. A.; Cheeseman, J. R.; Montgomery, Jr., J. A.; Vreven, T.; Kudin, K. N.; Burant, J. C.; Millam, J. M.; Iyengar, S. S.; Tomasi, J.; Barone, V.; Mennucci, B.; Cossi, M.; Scalmani, G.; Rega, N.; Petersson, G. A.; Nakatsuji, H.; Hada, M.; Ehara, M.; Toyota, K.; Fukuda, R.; Hasegawa, J.; Ishida, M.; Nakajima, T.; Honda, Y.; Kitao, O.; Nakai, H.; Klene, M.; Li, X.; Knox, J. E.; Hratchian, H. P.; Cross, J. B.; Bakken, V.; Adamo, C.; Jaramillo, J.; Gomperts, R.; Stratmann, R. E.; Yazyev, O.; Austin, A. J.; Cammi, R.; Pomelli, C.; Ochterski, J. W.; Ayala, P. Y.; Morokuma, K.; Voth, G. A.; Salvador, P.; Dannenberg, J. J.; Zakrzewski, V. G.; Dapprich, S.; Daniels, A. D.; Strain, M. C.; Farkas, O.; Malick, D. K.; Rabuck, A. D.; Raghavachari, K.; Foresman, J. B.; Ortiz, J. V.; Cui, Q.; Baboul, A. G.; Clifford, S.; Cioslowski, J.; Stefanov, B. B.; Liu, G.; Liashenko, A.; Piskorz, P.; Komaromi, I.; Martin, R. L.; Fox, D. J.; Keith, T.; Al-Laham, M. A.; Peng, C. Y.; Nanayakkara, A.; Challacombe, M.; Gill, P. M. W.; Johnson, B.; Chen, W.;

Wong, M. W.; Gonzalez, C.; and Pople, J. A. *Gaussian 03, Revision B.02*; Gaussian, Inc.: Wallingford, CT, 2004.

57. Becke, A. D. *J. Chem. Phys.* **1993**, *98*, 5648.
58. Lee, C.; Yang, W.; Parr, R. G. *Phys. Rev. B* **1988**, *37*, 785.
59. Hay, P. J.; Wadt, W. R. *J. Chem. Phys.* **1985**, *82*, 299.
60. (a) Hariharan, P. C.; Pople, J. A. *Theor. Chim. Acta* **1973**, *28*, 213. (b) Petersson, G. A.; Al-Laham, M. A. *J. Chem. Phys.* **1991**, *94*, 6081. (c) Petersson, G. A.; Bennett, A.; Tensfeldt, T. G.; Al-Laham, M. A.; Shirley, W. A.; Mantzaris, J. *J. Chem. Phys.* **1988**, *89*, 2193.
61. Portmann, S.; Lüthi, H. P.; *MOLEKEL: An Interactive Molecular Graphics Tool*. *CHIMIA* **2000**, *54*, 766.
62. Ortiz, J. C.; Bo, C. *Xaim*; Departamento de Química Física e Inorgánica, Universidad Rovira i Virgili: Tarragona, Spain, 1998.

(For Table of Contents Only)

Text for Table of Contents

Room-temperature reactions of the title complex with suitable precursors of carbonylic ML_n fragments (M = Mo, W, Fe) eventually result in P–P bond cleavage processes in the diphosphenyl ligand, to give trinuclear derivatives bridged by pyramidal phosphide and phosphinidene ligands, or by a trigonal planar phosphide ligand.

Graphics for Table of Contents